Neutrino collective excitations in the standard model at high temperature

D. Boyanovsky

Department of Physics and Astronomy, University of Pittsburgh, Pittsburgh, Pennsylvania 15260, USA

(Received 20 May 2005; published 5 August 2005)

Neutrino collective excitations are studied in the standard model at high temperatures below the symmetry breaking scale in the regime $T \gg M_{W,Z}(T) \gg gT$. Two parameters determine the properties of the collective excitations: a mass scale $m_\nu = gT/4$ which determines the *chirally symmetric* gaps in the spectrum and $\Delta = M_W^2(T)/2m_\nu T$. The spectrum consists of left-handed negative helicity quasiparticles, left-handed positive helicity quasiholes, and their respective antiparticles. For $\Delta < \Delta_c = 1.275\cdots$ there are two gapped quasiparticle branches and one gapless and two gapped quasihole branches, all but the higher gapped quasiparticle branches terminate at end points. For $\Delta_c < \Delta < \pi/2$ the quasiparticle spectrum features a pitchfork bifurcation and for $\Delta > \pi/2$ the collective modes are gapless quasiparticles with dispersion relation below the light cone for $k \ll m_\nu$ approaching the free field limit for $k \gg m_\nu$ with a rapid crossover between the soft nonperturbative to the hard perturbative regimes for $k \sim m_\nu$. The *decay* of the vector bosons leads to a *width* of the collective excitations of order g^2 which is explicitly obtained in the limits $k = 0$ and $k \gg m_\nu\Delta$. At high temperature this damping rate is shown to be competitive with or larger than the collisional damping rate of order G_F^2 for a wide range of neutrino energy.

DOI: 10.1103/PhysRevD.72.033004 PACS numbers: 13.15.+g, 11.10.Wx, 12.15.−y

I. INTRODUCTION

Neutrinos are emerging as the bridge between particle physics, astrophysics, cosmology, and nuclear physics. Physical processes involving neutrinos in dense and hot media are important from cosmology [1–7] to the astrophysics of compact stars [8–11]. More recently, it has been proposed that leptogenesis in the early Universe could be the main mechanism that explains the origin of the baryon asymmetry [12–14]. In this scenario the spectrum of neutrinos is an important ingredient that determines the size of the corrections in the transport equations for leptogenesis [14]. More refined studies of thermal leptogenesis include finite temperature corrections in the fermion propagators [15], which were previously found in vectorlike theories (QCD and QED) [16,17].

Neutrino propagation in hot and/or dense matter has become very important in astrophysics and cosmology after Wolfenstein [18] studied the effective potential and refractive index of neutrinos in matter and Mikheyev and Smirnov recognized the possibility that matter effects result in resonant flavor oscillations [19]. The MSW effect is now recognized to be the solution of the solar neutrino problem. The importance of medium effects in the propagation of neutrinos warrants an active program to study the possible cosmological and astrophysical consequences of novel dispersion relations and nonequilibrium aspects of neutrinos in hot and dense media.

Early studies of neutrino propagation in hot and/or dense media focused on the possible modifications of the neutrino dispersion relations in the regime of temperatures relevant for stellar evolution or for big bang nucleosynthesis, namely, up to ~1–10 MeV. Neutrino dispersion relations and damping rates in this regime of temperature has originally been obtained in Ref. [20] up to lowest order in the momentum dependence of the weak interactions in the standard model at temperatures well below the electroweak scale. Since then these results have been extended by several authors to include the corrections from light scalars [21], to study matter effects in the oscillations of neutrinos in the early Universe [6,22–24], and to a medium that includes nucleons, leptons, and neutrinos [25] as well as the relaxation (damping) rate of neutrinos in a hot and dense medium [6,20,22,26,27]. Damping rates and mean free paths of neutrinos in models beyond the standard model have been studied in Ref. [28].

While all of these thorough studies of the aspects of neutrino propagation focus on temperature (and chemical potential) scales suitable for primordial nucleosynthesis or stellar evolution, a systematic study of neutrino dispersion relations at high temperatures, near the *electroweak scale* has not (to the best of our knowledge) yet emerged.

Motivated to a large extent to explore the possibility of thermal leptogenesis in the standard model, as well as to study, in general, possible nonequilibrium aspects of neutrinos that could be relevant to lepto or baryogenesis [29] the purpose of this article is precisely to bridge this gap and study the propagation of neutrinos at high temperatures, near (but below) the electroweak scale *in the standard model*.

Since in the standard model baryon number and *CP* are not conserved it was conjectured that the cosmological baryon asymmetry could have been generated at the electroweak phase transition, if it was of first order. However a substantial body of work has revealed that for a Higgs mass larger than about 72 GeV there is a smooth crossover instead of a sharp transition [30]. The current CERN LEP bound for the standard model Higgs mass $m_H \gtrsim 115$ GeV

*Electronic address: boyan@pitt.edu

all but rules out the possibility of a strong first order phase transition and suggests a smooth crossover from the broken symmetry into the symmetric phase in the standard model. Supersymmetric extensions of the standard model may accommodate a strong first order phase transition, but we will focus our study on the standard model in this article.

The goal of this article.—We study the properties of neutrino collective excitations at high temperatures but below the symmetry breaking scale in the standard model. The focus is on obtaining the dispersion relations and damping rates of collective excitations of neutrinos in the medium by including the full momentum dependence in the contribution from the vector bosons.

If, as strongly suggested by the numerical analysis [30], the standard model has a smooth crossover between the broken and the unbroken symmetry phases, or even a second order phase transition, the expectation value of the neutral component of the scalar doublet diminishes monotonically as the symmetry breaking temperature scale is approached from below. In this case the mass of the vector bosons along with the (chiral symmetry breaking) masses for the leptons and quarks vanish continuously as the symmetry restoration temperature is approached from below.

Even when at finite temperature the non-Abelian vector bosons acquire a Debye (electric) mass $m_D \sim gT$ and a magnetic mass $m_m \sim g^2T$ [31–33], an important consequence is that there is a large abundance of vector bosons in the medium which enhances processes that are neglected at lower temperatures.

As it will be discussed in detail below some of these processes lead to a damping rate of collective excitations at lowest order in the weak coupling.

The propagation properties of neutrinos in a medium are obtained from an evaluation of the self-energy which takes into account the full propagator of the vector bosons up to one-loop order in the high temperature limit. The main assumptions that are used in our study are the following:

(i) We consider standard model neutrinos, namely, left-handed massless neutrinos with flavor number conservation. The study of neutrino mixing and oscillations will be presented elsewhere [34].

(ii) We study the high temperature regime below the symmetry breaking electroweak scale, $T_{\rm EW}$ in which the masses of the vector bosons $M_{W,H}(T) < <T < T_{\rm EW}$. The temperature dependence of the vector boson mass arises from the temperature dependence of the expectation value of the neutral scalar in the standard model scalar doublet. Under the assumption of a smooth crossover, as seems to be indicated by the lattice data, or of a second order transition, this expectation value monotonically diminishes as $T \to T_{\rm EW}$ from below. Since leptons and quarks obtain masses $m_f(T)$ via Yukawa couplings to the same scalar that gives the mass to the vector bosons the ratios remain almost constant, namely, $m_f(T)/M_{W,H}(T) \sim m_f(0)/M_{W,H}(0) \ll 1$. We neglect possible logarithmic variations of the weak and Yukawa couplings with temperature via the standard renormalization group running. Therefore at high temperature we will *neglect* the fermion masses in our analysis and will consider neutrinos and leptons to be massless.

(iii) We also consider a *CP* symmetric thermal bath, thereby neglecting contributions which are proportional to the baryon asymmetry of the Universe.

Brief summary of main results.—The main results obtained here are the following:

(i) We obtain the effective Dirac equations of neutrinos in the medium from a linear response approach. Under the assumption that in the standard model there is either a smooth crossover or a second order transition, we consider the regime of temperatures near but below the electroweak scale within which the mass of the vector bosons is much smaller than the temperature. In this regime we implement the hard thermal loop (HTL) approximation [17,31,32] and obtain the dispersion relations of neutrino collective excitations in the medium. It is argued that perturbation theory and the HTL approximation are reliable for $T \gg M_{W,Z}(T) \gg gT$.

(ii) In this regime, the properties of the neutrino collective modes are qualitative and quantitatively different from those of the fermionic excitations in QCD and QED [16,17,31,32] and depend on two parameters: a chirally symmetric mass scale $m_\nu = gT/4$ and the dimensionless combination $\Delta = M_W^2(T)/2m_\nu T$. Collective excitations are left-handed negative helicity quasiparticles and left-handed positive helicity quasiholes and their respective antiparticles. For $\Delta < \Delta_c = 1.275\cdots$ there are two gapped branches of quasiparticle excitations and one gapless and two gapped branches of quasihole excitations. The lower quasiparticle branch and *all* the quasihole branches terminate at end-point values of the momentum k determined by Δ while the dispersion relation of the upper gapped quasiparticle branch merges with the free field dispersion relation for $k \gg m_\nu$. For $\Delta_c < \Delta < \pi/2$ the quasiparticle spectrum features a pitchfork bifurcation and for $\Delta > \pi/2$ there are no quasihole branches available and only a gapless quasiparticle branch remains. Its dispersion relation is below the light cone for soft momenta $k \ll m_\nu$ and approaches the free field limit for $k \gg m_\nu\Delta$ with a sharp crossover between the nonperturbative and perturbative regimes at $k \sim m_\nu$.

(iii) Quasiparticles and quasiholes acquire a width as a result of the *decay* of vector bosons into neutrinos and leptons. This is a novel feature which distinguishes these excitations from those of high temperature QCD and QED and has a simple kinetic

interpretation. We obtain the damping rate for quasiparticles and quasiholes both at rest as well as for fast-moving excitations with $k \gg m_\nu \Delta$. These widths are of $\mathcal{O}(g^2)$ and it is argued that they can be larger than the collisional width of $\mathcal{O}(G_F^2)$ [20,26,27] at high temperature for momenta $k \lesssim M_W(T)$.

(iv) The domain of validity of the one-loop HTL approximation as well as the gauge invariance of the results are discussed in detail.

The article is organized as follows. In Sec. II we obtain the effective Dirac equation for neutrinos in the medium implementing a real-time approach in linear response. In Sec. III we study the one-loop self-energy in the HTL approximation. In Sec. III the spectrum of collective excitations and their damping rates are obtained. In this section we discuss the regime of validity of the HTL approximation and give a simple kinetic argument that shows that the decay of vector bosons implies a width for the collective excitations. Section VI is devoted to a discussion of the results and their gauge invariance as well as a comparison between the collisional damping rate of $\mathcal{O}(G_F^2)$ and the one-loop damping rate. Our conclusions and further questions are summarized in Sec. VII. An appendix provides the technical details for the self-energy.

II. THE EFFECTIVE DIRAC EQUATION IN THE MEDIUM

Anticipating a study of the real-time dynamics of neutrino propagation in a medium, including eventually mixing and oscillations [34], we obtain the real-time effective Dirac equations for neutrinos propagating in a thermal medium. While in this article we focus on standard model neutrinos, the generalization to include mixing, sterile, right handed, or Majorana neutrinos is straightforward.

The computation of the self-energy is carried out in the unitary gauge. This gauge reveals the correct physical degrees of freedom [35] and previous calculations of the neutrino self-energy in covariant gauges (one of which is the unitary gauge) have proven the gauge independence of the dispersion relations [25].

The part of the standard model Lagrangian density which is relevant to our discussion is the following:

$$\mathcal{L}_{\rm SM} = \overline{\nu}_a (i\not{\partial}) L \nu_a + \mathcal{L}^0_W + \mathcal{L}^0_Z + \mathcal{L}_{\rm CC} + \mathcal{L}_{\rm NC} \quad (2.1)$$

where $\mathcal{L}^0_{W,Z}$ are the free field Lagrangians for the vector bosons in unitary gauge, namely,

$$\mathcal{L}^0_W = -\frac{1}{2}(\partial_\mu W^+_\nu - \partial_\nu W^+_\mu)(\partial^\mu W^{-\nu} - \partial^\nu W^{-\mu}) + M^2_W W^+_\mu W^{-\mu}, \quad (2.2)$$

$$\mathcal{L}^0_Z = -\frac{1}{4}(\partial_\mu Z_\nu - \partial_\nu Z_\mu)(\partial^\mu Z^\nu - \partial^\nu Z^\mu) + \frac{1}{2} M^2_Z Z_\mu Z^\mu, \quad (2.3)$$

and the charged and neutral current interaction Lagrangian densities are given by

$$\mathcal{L}_{\rm CC} = \frac{g}{\sqrt{2}}[\overline{\nu}_a \gamma^\mu L l_a W^+_\mu + \overline{l}_a \gamma^\mu L \nu_a W^-_\mu], \quad (2.4)$$

$$\mathcal{L}_{\rm NC} = \frac{g}{2\cos\theta_w}[\overline{\nu}_a \gamma^\mu L \nu_a Z_\mu + \overline{f}_a \gamma^\mu (g^V_a - g^A_a \gamma^5) f_a Z_\mu]. \quad (2.5)$$

In the above expressions $L = (1 - \gamma^5)/2$ is the projection operator on left-handed states, a is a flavor index, and $g^{V,A}$ are the vector and axial vector couplings of quarks and leptons. l stand for leptons and f generically for the fermion species with neutral current interactions.

The effective Dirac equation in the medium in real time is derived in linear response by implementing the methods of nonequilibrium quantum field theory described in Ref. [36]. In this approach an external source induces an expectation value for the neutrino field and this expectation value obeys the effective equation of motion in the medium, including self-energy contributions [36]. This approach allows the study of the real-time dynamics as an *initial value problem* which will be a distinct advantage to study neutrino oscillations in the medium.

To implement this approach we introduce an external Grassmann-valued source that couples linearly to the neutrino field via the Lagrangian density

$$\mathcal{L}_S = \overline{\nu}_a \eta_a + \overline{\eta}_a \nu_a. \quad (2.6)$$

In presence of this source term, the total Lagrangian density is given by $\mathcal{L}_{\rm SM} + \mathcal{L}_S$.

The calculation of *expectation values* (rather than in-out S-matrix elements) requires the generating function of real-time correlation functions, which involves evolution along forward and backward time branches [37]. A path integral representation of this generating functional is given by

$$\mathcal{Z}[j^+, j^-] = \int D\Phi^+ D\Phi^- e^{i\int (\mathcal{L}[\Phi^+, j^+] - \mathcal{L}[\Phi^-, j^-])} \quad (2.7)$$

where we have generically denoted by $\Phi^\pm$ *all* the fields defined along the forward $(+)$ and backward $(-)$ time branches to facilitate the notation. The sources $j^\pm$ are linearly coupled to these fields in order to obtain the real-time correlation functions as functional derivatives of the generating functional with respect to these sources. While the sources $j^\pm$ are introduced to obtain the real-time correlation functions and are set to zero after the calculations, the external (Grassman) source η is the same along both branches $\pm$ and induces an expectation value of the neutrino field which is the same along both branches. See

Refs. [36–39] for further discussion. The equation of motion for the expectation value of the neutrino field induced by the external source is obtained by shifting the field

$$\nu_a^{\pm} = \chi_a + \Psi_a^{\pm}; \qquad \chi_a = \langle \nu_a^{\pm} \rangle; \qquad \langle \Psi_a^{\pm} \rangle = 0. \quad (2.8)$$

The equation of motion for the expectation value is obtained by requesting that the $\langle \Psi_a^{\pm} \rangle = 0$ be fulfilled order by order in perturbation theory [38,39]. Implementing this method up to one-loop order we find the following equation of motion [36]:

$$i(\not{\partial}) L \chi_a(\vec{x}, t) + \int d^3x' \int dt' \Sigma^{\rm ret}_{ab}(\vec{x} - \vec{x}', t - t') \chi_b(\vec{x}', t') = -\eta_a(\vec{x}, t) \quad (2.9)$$

where $\Sigma^{ret}_{ab}(\vec{x} - \vec{x}', t - t')$ is the retarded self-energy in real time whose one-loop contributions are displayed in Fig. 1. In this study we will consider only a *CP* symmetric medium; therefore we neglect the neutral current one-loop tadpole diagrams with a closed neutrino or lepton loop and only the one-loop diagrams with the exchange of charged or neutral vector bosons is considered, namely, the two top diagrams in Fig. 1.

The one-loop contributions from vector boson exchange to the retarded self-energy are computed in the appendix. It is convenient to introduce the space-time Fourier transform of the expectation value and the source

$$\chi_a(\vec{x}, t) = \frac{1}{\sqrt{V}} \sum_{\vec{k}} \int d\omega \chi_a(\vec{k}, \omega) e^{i\vec{k}\cdot\vec{x}} e^{-i\omega t}; \qquad \eta_a(\vec{x}, t) = \frac{1}{\sqrt{V}} \sum_{\vec{k}} \int d\omega \eta_a(\vec{k}, \omega) e^{i\vec{k}\cdot\vec{x}} e^{-i\omega t} \quad (2.10)$$

where we have kept the same name for the variables to avoid introducing further notation.

Since we are considering the high temperature limit with T much larger than the lepton masses (only the lightest leptons are considered) we neglect the fermion masses in the computation of the self-energy. As it will become clear from the discussion below, this is warranted because in the high temperature limit the loop momentum is of order T. In this case the self-energies are proportional to the identity matrix in flavor space. Using the results of the appendix, the equation of motion in frequency and momentum for each individual flavor becomes

$$[\gamma^0 \omega - \vec{\gamma} \cdot \vec{k} + \Sigma_W(\vec{k}, \omega) + \Sigma_Z(\vec{k}, \omega)] L \chi_a(\vec{k}, \omega) = -\eta_a(\vec{k}, \omega). \quad (2.11)$$

The one-loop contribution to the self-energies $\Sigma_{W,Z}(\vec{k}, \omega)$ are given by the first two diagrams in Fig. 1. The details of their calculation is presented in the appendix and their final expressions are given by Eq. (A29) in terms of the dispersive forms (A26) and (A27).

III. THE SELF-ENERGY: CHARGED AND NEUTRAL CURRENTS

From the results of the appendix, in particular, Eqs. (A29) and (A30), we obtain the following explicit expression for the self-energies:

$$\Sigma_{W,Z}(\vec{k}, \omega) = \int \frac{dk_0}{\pi} \frac{{\rm Im}\Sigma_{W,Z}(\vec{k}, k_0)}{k_0 - \omega - i\epsilon}, \quad (3.1)$$

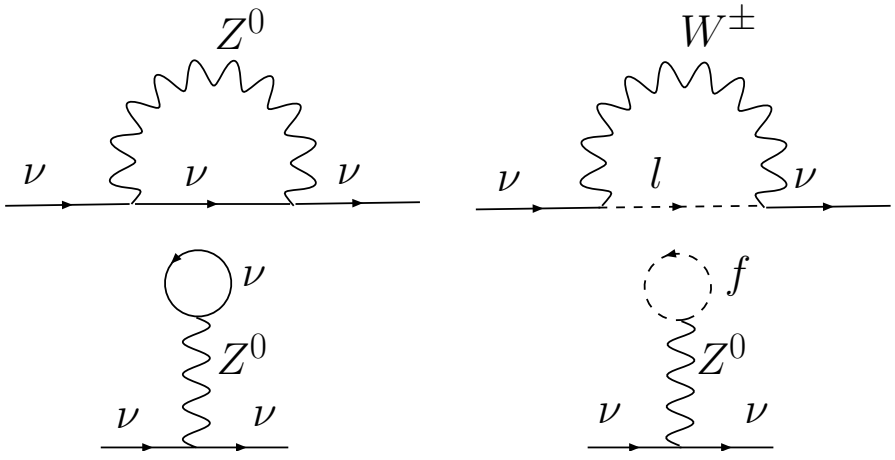

FIG. 1. One-loop diagrams contributing to the neutrino self-energy. The tadpole diagrams (neutral currents) with neutrino and lepton loops are not considered in the case of a *CP* symmetric medium.

$$\begin{aligned}\mathrm{Im}\,\Sigma_W(\vec{k},k_0) = \frac{g^2\pi}{2}\int\frac{d^3q}{(2\pi)^3}\frac{1}{4W_q p}\{&[1-N_f(p)\\ &+N_b(W_q)][\mathcal{Q}(\vec{p},\vec{q})\delta(k_0-p-W_q)\\ &+\mathcal{Q}(-\vec{p},-\vec{q})\delta(k_0+p+W_q)]\\ &+[N_f(p)+N_b(W_q)][\mathcal{Q}(\vec{p},-\vec{q})\delta(k_0-p\\ &+W_q)+\mathcal{Q}(-\vec{p},\vec{q})\delta(k_0+p-W_q)]\}\end{aligned} \tag{3.2}$$

where

$$Q^\mu(\vec{p},\vec{q}) = p^\mu + 2q^\mu\left(\frac{W_q p-\vec{q}\cdot\vec{p}}{M_W^2(T)}\right), \tag{3.3}$$

$$p^\mu = (|\vec{k}-\vec{q}|,\vec{k}-\vec{q}), \tag{3.4}$$

$$q^\mu = (W_q,\vec{q}), \tag{3.5}$$

$$W_q = \sqrt{q^2+M_W^2(T)}. \tag{3.6}$$

The contribution from neutral currents is obtained from the above expression by the replacement

$$\frac{g}{\sqrt{2}}\to\frac{g}{2\cos\theta_w};\qquad M_W(T)\to M_Z(T)=\frac{M_W(T)}{\cos\theta_w}. \tag{3.7}$$

In what follows we will use the standard model value $\sin^2\theta_w = 0.23$ for numerical analysis, neglecting possible finite temperature corrections.

The delta functions in the expression for (3.2) (and similarly for the neutral current contribution) have a clear interpretation: those of the form $\delta(p+W_q\mp k_0)$ correspond to the process of *decay* of a neutrino (positive or negative energy) into an (anti) lepton and a vector boson and the inverse process of recombination. These processes remain at zero temperature but they imply a production threshold that can *only* be satisfied if the neutrino features a *gap* in its spectrum with a value larger than the mass of the vector bosons. The delta functions of the form $\delta(W_q - p\mp k_0)$ correspond to the processes of vector boson decay into a neutrino-(anti) lepton pair and its inverse (recombination) process. These processes are only available in the medium and their contribution vanishes in the zero temperature limit.

The form of the imaginary part of the self-energies suggests that the full self-energies can be written as follows:

$$\Sigma_{W,Z}(\vec{k},\omega) = \gamma^0\sigma^0_{W,Z}(k,\omega) - \vec{\gamma}\cdot\hat{\mathbf{k}}\,\sigma^1_{W,Z}(k,\omega). \tag{3.8}$$

The corresponding scalar functions $\sigma^0_{W,Z}(k,\omega)$, $\sigma^1_{W,Z}(k,\omega)$ are obtained by projection. Their explicit expression is given by

$$\begin{aligned}\mathrm{Im}\sigma^0_W(k_0,k) = \frac{g^2\pi}{2}\int\frac{d^3q}{(2\pi)^3}\frac{1}{4W_q p}\{&[1-N_f(p)+N_b(W_q)]Q_0(\vec{p},\vec{q})[\delta(k_0-p-W_q)+\delta(k_0+p+W_q)]\\ &+[N_f(p)+N_b(W_q)]Q_0(\vec{p},-\vec{q})[\delta(k_0-p+W_q)+\delta(k_0+p-W_q)]\},\end{aligned} \tag{3.9}$$

$$\begin{aligned}\mathrm{Im}\sigma^1_W(k_0,k) = \frac{g^2\pi}{2}\int\frac{d^3q}{(2\pi)^3}\frac{1}{4W_q p}\{&[1-N_f(p)+N_b(W_q)]\hat{\mathbf{k}}\cdot\vec{Q}(\vec{p},\vec{q})[\delta(k_0-p-W_q)-\delta(k_0+p+W_q)]\\ &+[N_f(p)+N_b(W_q)]\hat{\mathbf{k}}\cdot\vec{Q}(\vec{p},-\vec{q})[\delta(k_0-p+W_q)-\delta(k_0+p-W_q)]\}.\end{aligned} \tag{3.10}$$

Using the dispersive representation (3.1) we find the following expressions:

$$\begin{aligned}\sigma^0_W(\omega,k) = \frac{g^2}{2}\int\frac{d^3q}{(2\pi)^3}\frac{1}{4W_q p}\Big\{&[1-N_f(p)+N_b(W_q)]Q_0(\vec{p},\vec{q})\left[\frac{1}{p+W_q-\omega-i\epsilon}-\frac{1}{p+W_q+\omega+i\epsilon}\right]\\ &+[N_f(p)+N_b(W_q)]Q_0(\vec{p},-\vec{q})\left[\frac{1}{p-W_q-\omega-i\epsilon}-\frac{1}{p-W_q+\omega+i\epsilon}\right]\Big\},\end{aligned} \tag{3.11}$$

$$\begin{aligned}\sigma^1_W(\omega,k) = \frac{g^2}{2}\int\frac{d^3q}{(2\pi)^3}\frac{1}{4W_q p}\Big\{&[1-N_f(p)+N_b(W_q)]\hat{\mathbf{k}}\cdot\vec{Q}(\vec{p},\vec{q})\left[\frac{1}{p+W_q-\omega-i\epsilon}+\frac{1}{p+W_q+\omega+i\epsilon}\right]\\ &+[N_f(p)+N_b(W_q)]\hat{\mathbf{k}}\cdot\vec{Q}(\vec{p},-\vec{q})\left[\frac{1}{p-W_q-\omega-i\epsilon}+\frac{1}{p-W_q+\omega+i\epsilon}\right]\Big\}.\end{aligned} \tag{3.12}$$

The expressions for the neutral current contributions can be obtained by the simple replacement (3.7) and adding both contributions defines the following scalar functions:

$$\sigma^0(\omega, k) = \sigma^0_W(\omega, k) + \sigma^0_Z(\omega, k);$$
$$\sigma^1(\omega, k) = \sigma^1_W(\omega, k) + \sigma^1_Z(\omega, k). \tag{3.13}$$

An important property of the imaginary parts that will be useful in the analysis of the width of the collective modes is the following:

$$\mathrm{Im}\,\sigma^0(-\omega, k) = \mathrm{Im}\sigma^0(\omega, k), \tag{3.14}$$

$$\mathrm{Im}\,\sigma^1(-\omega, k) = -\mathrm{Im}\sigma^1(\omega, k). \tag{3.15}$$

A. Hard thermal loops

In the high temperature limit $T \gg M_{W,Z}(T)$ the integrands in the expressions above are dominated by loop momentum $q \sim T$. This is simply gleaned from the high powers of momentum that multiply the Fermi-Dirac and Bose-Einstein distribution functions. In this limit, the HTL approximation[17,31,32] is warranted. For frequency and momentum of the neutrino excitations $k, \omega \ll T$ the HTL "counting" $q \sim T \gg k, \omega$ leads to the following approximations:

$$p \sim q - \vec{k}\cdot\hat{\mathbf{q}}; \qquad W_q \sim q + \frac{M^2}{2q}, \tag{3.16}$$

where M stands generically for $M_{W,Z}(T)$.

Ignoring the vacuum contribution, a lengthy but straightforward calculation using these approximations leads to the following results for the real parts:

$$\mathrm{Re}\,\sigma^0_W(k, \omega) = \frac{m^2_\nu \omega}{12M^2_W(T)} - \frac{m^2_\nu}{2k} I(\omega, k, \Delta), \tag{3.17}$$

$$\mathrm{Re}\,\sigma^1_W(k, \omega) = -\frac{m^2_\nu k}{18M^2_W(T)} + \frac{m^2_\nu}{2k} J(\omega, k, \Delta) \tag{3.18}$$

where

$$m_\nu = \frac{gT}{4}. \tag{3.19}$$

The dimensionless functions $I(\omega, k)$ and $J(\omega, k)$ are more compactly expressed by introducing the dimensionless variables

$$\overline{\omega} = \frac{\omega}{m_\nu}; \qquad \overline{k} = \frac{k}{m_\nu}, \tag{3.20}$$

$$\Delta = \frac{M^2_W(T)}{2m_\nu T} = \frac{g}{8}\left(\frac{M_W(T)}{m_\nu}\right)^2 \tag{3.21}$$

and the functions

$$LP(\overline{\omega}, \overline{k}, \Delta; z) = \frac{1}{2}\ln\left|\frac{\overline{\omega} + \overline{k} + \frac{\Delta}{z}}{\overline{\omega} - \overline{k} + \frac{\Delta}{z}}\right|, \tag{3.22}$$

$$LM(\overline{\omega}, \overline{k}, \Delta; z) = \frac{1}{2}\ln\left|\frac{\overline{\omega} + \overline{k} - \frac{\Delta}{z}}{\overline{\omega} - \overline{k} - \frac{\Delta}{z}}\right|, \tag{3.23}$$

in terms of which

$$I(\omega, k, \Delta) = \frac{4}{\pi^2}\int_0^\infty dz \frac{2ze^{-z}}{1 - e^{-2z}}[LP(\overline{\omega}, \overline{k}, \Delta; z) + LM(\overline{\omega}, \overline{k}, \Delta; z)], \tag{3.24}$$

$$J(\omega, k, \Delta) = \frac{4}{\pi^2}\int_0^\infty dz \frac{2ze^{-z}}{1 - e^{-2z}} \times\left[2 - \frac{\overline{\omega} + \frac{\Delta}{z}}{\overline{k}} LP(\overline{\omega}, \overline{k}, \Delta; z) - \frac{\overline{\omega} - \frac{\Delta}{z}}{\overline{k}} LM(\overline{\omega}, \overline{k}, \Delta; z)\right]. \tag{3.25}$$

Similar expressions are obtained for the neutral current contributions by the replacement (3.7). Adding together the charged and neutral current contributions leads to

$$I_T(\omega, k, \Delta) = I(\omega, k, \Delta) + \frac{1}{2\cos^2\theta_w} I\left(\omega, k, \frac{\Delta}{\cos^2\theta_w}\right), \tag{3.26}$$

$$J_T(\omega, k, \Delta) = J(\omega, k, \Delta) + \frac{1}{2\cos^2\theta_w} J\left(\omega, k, \frac{\Delta}{\cos^2\theta_w}\right). \tag{3.27}$$

We note that for $M_W = 0$

$$I(\omega, k, 0) = \ln\left|\frac{\omega + k}{\omega - k}\right|, \tag{3.28}$$

$$J(\omega, k, 0) = 2 - \frac{\omega}{k}\ln\left|\frac{\omega + k}{\omega - k}\right|, \tag{3.29}$$

which are the standard results of the HTL approximation for vectorlike theories without spontaneous symmetry breaking (QCD-QED) [17,31,32]. The following properties of these functions will be important in the discussion of the collective modes below,

$$I(-\omega, k, \Delta) = -I(\omega, k, \Delta), \tag{3.30}$$

$$J(-\omega, k, \Delta) = J(\omega, k, \Delta), \tag{3.31}$$

$$I(\omega, -k, \Delta) = -I(\omega, k, \Delta), \tag{3.32}$$

$$J(\omega, -k, \Delta) = J(\omega, k, \Delta), \tag{3.33}$$

$$J(\omega, 0, \Delta) = 0. \tag{3.34}$$

IV. DISPERSION RELATIONS AND WIDTHS OF COLLECTIVE EXCITATIONS

The form of the self-energies (3.8) allow one to write the *homogeneous* Dirac equation (setting to zero the external Grassmann sources η) in the form

$$[\Lambda_+(\hat{\mathbf{k}})D_-(\omega,k)+\Lambda_-(\hat{\mathbf{k}})D_+(\omega,k)]L\chi_a(\vec{k},\omega)=0 \tag{4.1}$$

where

$$\Lambda_\pm(\hat{\mathbf{k}})=\frac{1}{2}(\gamma^0\mp\vec{\gamma}\cdot\hat{\mathbf{k}})=\frac{\gamma^0}{2}(1\mp h(\hat{\mathbf{k}})\gamma^5). \tag{4.2}$$

Here $h(\hat{\mathbf{k}})$ is the helicity operator, and

$$D_+(\omega,k)=\omega-k+\sigma^0(k,\omega)-\sigma^1(k,\omega), \tag{4.3}$$

$$D_-(\omega,k)=\omega+k+\sigma^0(k,\omega)+\sigma^1(k,\omega). \tag{4.4}$$

Therefore, the propagator for left-handed fields is given by

$$iS(\omega,k)=\frac{\Lambda_+(\hat{\mathbf{k}})}{D_+(\omega,k)}+\frac{\Lambda_-(\hat{\mathbf{k}})}{D_-(\omega,k)}. \tag{4.5}$$

The neutrino spectral function is determined from the propagator above, and is given by

$$\begin{aligned}\rho(\omega,k)&=-\frac{1}{\pi}\,\mathrm{Im}[iS(\omega+i\epsilon,k)]\\&=\Lambda_+(\hat{\mathbf{k}})\rho_+(\omega,k)+\Lambda_-(\hat{\mathbf{k}})\rho_-(\omega,k)\end{aligned} \tag{4.6}$$

where

$$\rho_\pm(\omega,k)=\frac{1}{\pi}\frac{\mathrm{Im}D_\pm(\omega+i\epsilon,k)}{[\mathrm{Re}D_\pm(\omega+i\epsilon,k)]^2+[\mathrm{Im}D_\pm(\omega+i\epsilon,k)]^2}. \tag{4.7}$$

The poles of the propagator along the real axis in the complex ω plane correspond to physical stable excitations, while complex poles very near the real axis in a second (or higher) Riemann sheet in this plane describe quasiparticles or resonances. Propagating quasiparticles are characterized by narrow width resonances; namely, their widths must be much smaller than the real part of the (complex) pole, so the decay rate of the quasiparticle is much smaller than its oscillation frequency.

The position of the (quasi) particle poles are $\omega_\pm(k)$ which are determined by the conditions

$$\mathrm{Re}\,D_+(\omega_+(k),k)=0, \tag{4.8}$$

$$\mathrm{Re}\,D_-(\omega_-(k),k)=0. \tag{4.9}$$

If these functions vanish *linearly* near their zeroes, then near the resonances the spectral density can be approximated by a Breit-Wigner form, namely,

$$\rho_\pm(\omega,k)\sim\frac{Z_\pm(k)}{\pi}\frac{\Gamma_\pm(k)}{(\omega-\omega_\pm(k))^2+\Gamma_\pm^2(k)} \tag{4.10}$$

where the residues $Z_\pm(k)$ and widths (damping rates) $\Gamma_\pm(k)$ are given by

$$Z_\pm^{-1}(k)=\left|\frac{\partial D_\pm(\omega,k)}{\partial\omega}\right|_{\omega=\omega_\pm(k)}, \tag{4.11}$$

$$\Gamma_\pm(k)=Z_\pm(k)\mathrm{Im}D_\pm(\omega_\pm(k),k). \tag{4.12}$$

The spinor wave functions of the resonances (quasiparticles) are obtained from the homogeneous effective Dirac equation in the medium (4.1) by considering only the real part of $D_\pm(\omega,k)$, since the vanishing of the real parts defines the quasiparticles. Because neutrinos are left-handed fields the eigenspinors corresponding to the solutions of $D_+(\omega_+(k),k)=0$ must obey

$$(1+h(\hat{\mathbf{k}}))L\chi(\omega_+(k),k)=0. \tag{4.13}$$

Namely, the spinor eigenstate is a left-handed, negative helicity state, just as the usual neutrino field. We will refer to the *positive energy* solutions of $D_+(\omega_+(k),k)=0$ as *quasiparticles*. Similarly, the spinors' solutions corresponding to the roots of $D_-(\omega_-(k),k)=0$ must obey

$$(1-h(\hat{\mathbf{k}}))L\chi(\omega_-(k),k)=0, \tag{4.14}$$

corresponding to a left-handed neutrino state with *positive* helicity. Following Ref. [17], we will refer to the *positive energy* solutions of $D_-(\omega_-(k),k)=0$ as *quasiholes*. These states feature the *opposite* chirality-helicity assignment of the vacuum neutrino states.

As it will be discussed in detail in Sec. V, the regime of validity of the perturbative expansion is restricted to $M_{W,Z}(T)\gg gT$ in which case $m_\nu/M_{W,Z}(T)\ll 1$. Therefore the first terms in Eqs. (3.17) and (3.18) provide a perturbative correction to the coefficients of ω and k in $D_\pm(\omega,k)$. Since the focus is to explore the nonperturbative aspects of "soft" collective excitations we will ignore these terms in what follows. The final expressions for $D_\pm(\omega,k)$ are given by

$$\begin{aligned}D_+(\omega,k)=\omega-k-\frac{m_\nu^2}{2k}[I_T(\omega,k)+J_T(\omega,k)]\\+i[\mathrm{Im}\sigma^0(\omega,k)-\mathrm{Im}\sigma^1(\omega,k)],\end{aligned} \tag{4.15}$$

$$\begin{aligned}D_-(\omega,k)=\omega+k-\frac{m_\nu^2}{2k}[I_T(\omega,k)-J_T(\omega,k)]\\+i[\mathrm{Im}\sigma^0(\omega,k)+\mathrm{Im}\sigma^1(\omega,k)].\end{aligned} \tag{4.16}$$

The real and imaginary parts of $D_\pm(\omega,k)$ feature the following symmetries:

$$\mathrm{Re}\,D_+(-\omega,k)=-\mathrm{Re}D_-(\omega,k), \tag{4.17}$$

$$\mathrm{Im}\,D_+(-\omega,k)=\mathrm{Im}D_-(\omega,k). \tag{4.18}$$

The dispersion relations of quasiparticles and quasiholes are obtained from roots of the real part of the self-energy, namely,

$$\mathrm{Re}\, D_{\pm}(\omega_{\pm}(k), k) = 0. \tag{4.19}$$

The symmetry relation (4.17) indicates that we only need to find the *positive* roots in Eq. (4.19); therefore the roots of $\mathrm{Re}D_{\pm}(\omega, k) = 0$ will be the pairs $(\omega_{+}(k), -\omega_{-}(k)); (\omega_{-}(k); -\omega_{+}(k))$, respectively, with $\omega_{\pm}(k) \geq 0$.

Antiquasiparticles and antiquasiholes have negative energy and quantum numbers opposite to those of quasiparticles and quasiholes. The interpretation of the excitation spectrum is as follows [17]: the positive energy roots of $D_{+}(\omega, k)$ correspond to negative helicity left-handed *quasiparticle* states of energy $\omega_{+}(k)$ and spectral weight $Z_{+}(k)$ while the negative energy roots are left-handed *antiquasihole* states of negative helicity of energy $-\omega_{-}(k)$ and residue $Z_{-}(k)$. The positive energy roots of $D_{-}(\omega, k)$ correspond to left-handed positive helicity *quasiholes* of energy $\omega_{-}(k)$ and spectral weight $Z_{-}(k)$ and the negative energy roots correspond to left-handed positive helicity *antiquasiparticles* of energy $-\omega_{+}(k)$ and residue $Z_{+}(k)$. The relation between the imaginary parts, Eq. (4.18) states that quasiparticles and antiquasiparticles have the same width and so do quasiholes and antiquasiholes; this is obviously a consequence of the underlying *CPT* symmetry.

The table below summarizes the properties of the collective excitations [17].

Identity	E	h	Z	$\Gamma(k)$
quasiparticle	$\omega_{+}(k)$	-1	$Z_{+}(k)$	$\Gamma_{+}(k)$
antiquasiparticle	$-\omega_{+}(k)$	1	$Z_{+}(k)$	$\Gamma_{+}(k)$
quasihole	$\omega_{-}(k)$	1	$Z_{-}(k)$	$\Gamma_{-}(k)$
antiquasihole	$-\omega_{-}(k)$	-1	$Z_{-}(k)$	$\Gamma_{-}(k)$

A. Gaps in the spectrum of collective modes

The position of the gaps in the spectrum of collective excitations are determined by the roots of the equation

$$\mathrm{Re}\, D_{\pm}(\omega, k = 0, \Delta) = 0 \tag{4.20}$$

where we have used the property $J(\omega, k = 0) = 0$ [see Eq. (3.34)] which implies that $D_{+}(\omega, k = 0, \Delta) = D_{-}(\omega, k = 0, \Delta)$. General features of the gap equation (4.20) can be understood from the expression

$$D_{+}(\omega, 0, \Delta) = m_{\nu}\left\{\overline{\omega} + \frac{1}{2}\left[H(\overline{\omega}, \Delta) + \frac{1}{2\cos^2\theta_w} H\left(\overline{\omega}, \frac{\Delta}{\cos^2\theta_w}\right)\right]\right\} \tag{4.21}$$

where

$$H(\overline{\omega}, \Delta) = \frac{8\overline{\omega}}{\pi^2}\int_0^{\infty} dz\, \frac{2ze^{-z}}{1 - e^{-2z}}\, \mathcal{P}\left(\frac{1}{(\Delta^2/z^2) - \overline{\omega}^2}\right) \tag{4.22}$$

and $\mathcal{P}$ stands for the principal part.

For $\Delta = 0$, $H(\omega, 0) = -2\mathcal{P}(1/\omega)$ which leads to the solution of the gap equation

$$\omega(k = 0) = \pm m_{\nu}\left(1 + \frac{1}{2\cos^2\theta_w}\right)^{1/2}. \tag{4.23}$$

We note that because $\mathcal{P}(1/\omega)$ is an *odd* function of ω vanishing at $\omega = 0$ (by definition of the principal part) there are *three* roots of the equation $D_{+}(\omega, 0, 0) = 0$: $\omega = 0$ and the two roots corresponding to the value of the gap (4.23). The gapless excitations associated with the root $\omega = 0$ will be explored in Sec. IV C below for general values of Δ including $\Delta = 0$.

For $\Delta \neq 0$ the function $D_{+}(\omega = 0, k = 0, \Delta) = 0$ because it is an odd function of ω. Furthermore, for $\Delta \ll 1$ and $\omega \approx 0$, it follows that

$$H(\omega, \Delta) \sim \frac{\omega}{\Delta^2}. \tag{4.24}$$

Therefore, for $\Delta \neq 0$, $D_{+}(\omega, k = 0, \Delta)$ vanishes at $\omega = 0$, is positive for $\omega > 0$, and rises sharply from the origin with a slope $\propto 1/\Delta^2$. For small Δ the function $H(\omega, \Delta)$ eventually becomes negative for large enough ω. This is because the integrand is sharply peaked at $z \sim 2$; therefore, for sufficiently small Δ and sufficiently large ω the region in which the denominator is negative dominates. Since for large ω, $D_{+}(\omega, \Delta) \approx \omega$ there must be yet another sign change and the function $D_{+}(\omega, \Delta)$ must have at least *three zeroes*, namely, three roots. One of the roots corresponds to $\omega = 0$ which determines a *gapless* branch of collective excitations; however, for small Δ one of the roots must be at $\overline{\omega} \sim \Delta$ while another root should be at $\overline{\omega} \sim (1 + \frac{1}{2\cos^2\theta_w})^{1/2}$. Therefore for $\Delta \ll 1$ there are *three* branches; one emerging from the origin is gapless and two other branches feature a gap in their dispersion relations.

However, for larger Δ the region in which the denominator becomes negative necessarily corresponds to $z > > 2$ and the integrand is strongly suppressed in which case the function $H(\omega, \Delta)$ will always be positive and no root will be available. This behavior is clearly displayed in Fig. 2 where we used the standard model value $\sin^2\theta_w = 0.23$.

This figure shows that there is a *critical value* Δ_c such that for $\Delta \lesssim \Delta_c$ there are *two* nonvanishing roots which coalesce at $\Delta = \Delta_c$ while for $\Delta > \Delta_c$ the only root available is $\omega = 0$. We find numerically that the critical value is given by

$$\Delta_c \sim 1.275 \cdots. \tag{4.25}$$

In order to resolve whether the gapless branch describes quasiparticles or quasiholes, we must find the k dependence of the gapless branch.

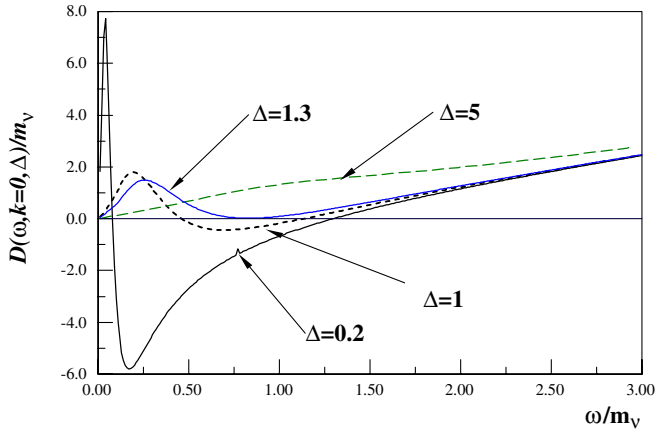

FIG. 2 (color online). Roots of $D(\omega, k = 0, \Delta)$ for $\Delta = 0.2$, 1, 1.3, 5, respectively. The intersection of these lines with the horizontal axis determines the values of the gap in the spectra of collective modes.

A straightforward but lengthy calculation shows that to linear order in k

$$D_{\pm}(\omega, k, \Delta) = D_{+}(\omega, 0, \Delta) \mp k\Big[1 + S(\overline{\omega}, \Delta) + \frac{1}{2\cos^2\theta_w} S\Big(\overline{\omega}, \frac{\Delta}{\cos^2\theta_w}\Big)\Big] \tag{4.26}$$

with $D_{+}(\overline{\omega}, 0, \Delta)$ given by Eq. (4.21) and

$$S(\overline{\omega}, \Delta) = -\frac{4}{3\pi^2}\int_0^\infty dz \frac{2ze^{-z}}{1 - e^{-2z}} \mathcal{P}\Big[\frac{(\Delta^2/z^2) + \overline{\omega}^2}{((\Delta^2/z^2) - \overline{\omega}^2)^2}\Big]. \tag{4.27}$$

Therefore the dispersion relations for small k near the gaps with value $\omega_{\pm}(0)$ are given by

$$\omega_{\pm}(k) \sim \omega_{\pm}(0) + c_{\pm}k + \mathcal{O}(k^2) \tag{4.28}$$

with the group velocities $c_{\pm}$ given by

$$c_{\pm} = \pm\frac{1}{D'(\omega_{\pm}(0), 0, \Delta)}\Big[1 + S(\overline{\omega}_{\pm}(0), \Delta) + \frac{1}{2\cos^2\theta_w} S(\overline{\omega}_{\pm}(0), \frac{\Delta}{\cos^2\theta_w})\Big]. \tag{4.29}$$

Therefore for sufficiently small k *all* branches of collective modes behave linearly with k. The study of the group velocities for each branch necessarily has to be done numerically; however of particular interest is the group velocity for long-wavelength excitations of the *gapless* branch. A straightforward calculation for $\omega_{\pm}(0) = 0$ leads to the following result:

$$c_{\pm} = \pm\Big[\frac{\Delta^2 - (\pi^2/4)}{\Delta^2 + (3\pi^2/4)}\Big] \tag{4.30}$$

where $\pm$ refer to the roots of $D_{\pm}(\omega, k, \Delta)$, respectively. As discussed above, quasiparticles and quasiholes are *positive energy* roots of $D_{\pm}(\omega, k, \Delta)$, respectively. Hence, the expression for the group velocity for long-wavelength excitations on the gapless branch (4.30) indicates that for $\Delta < \pi/2$ positive energy excitations on the gapless branch are *quasiholes*, while for $\Delta > \pi/2$ gapless collective modes are *quasiparticles*. Therefore the gapless branch changes identity at $\Delta = \pi/2$.

In summary, the spectrum of collective excitations always features a *gapless* branch for any value of Δ. For $\Delta < \pi/2$ these gapless collective modes are quasiholes, and for $\Delta > \pi/2$ they are quasiparticles.

For generic $\Delta < \Delta_c \sim 1.275\cdots$ the quasiparticle spectrum will feature at least two gapped branches, while the quasihole spectrum will feature two gapped and one gapless branch. For $\Delta \ll 1$ the lowest gapped branch begins at $|\omega(0)| \sim \Delta$ while the highest one begins at $|\omega(0)| \sim m_\nu(1 + \frac{1}{2\cos^2\theta_w})^{1/2}$. For $\Delta > \pi/2$ the quasiparticle spectrum only features a gapless branch and no branches of collective excitations remain for quasiholes.

The dispersion relations are linear for small momentum k in each branch. However, the gapless branch corresponds to roots of $D_{-}(\omega, k, \Delta)$ for $\Delta < \pi/2$ while it describes the *only* available gapless branch of $D_{+}(\omega, k, \Delta)$ for $\Delta > \pi/2$. A detailed numerical analysis of the quasiparticle and quasihole collective modes is presented below.

B. Quasiparticle spectrum

The dispersion relation of quasiparticles corresponds to the positive roots of $\mathrm{Re}D_{+}(\omega_{+}(k), k, \Delta)$. The study of the dispersion relation in the full range of k and Δ must necessarily be carried out numerically. However, before doing so, we can gain insight into the nature of the dispersion relations by considering the simplified case of $\Delta = 0$. While this case is outside the domain of validity of the perturbative expansion because of the restriction that $M_{W,Z}(T) \gg m_\nu$ (see Sec. V), the study of this case highlights several relevant aspects of the dispersion relation and also serves as comparison to the more familiar results in the literature in the case of unbroken gauge theories in the HTL approximation [17,31,32].

In the case $\Delta = 0$ the function $D_{+}(\omega, k, 0)$ is familiar from the HTL approximation for fermionic excitations in unbroken vectorlike gauge theories [17,31,32]

$$D_{+}(\omega, k, 0) = m_\nu\Big\{\overline{\omega} - \overline{k} + \frac{C}{2\overline{k}}\Big[\Big(1 - \frac{\overline{\omega}}{\overline{k}}\Big)\ln\Big|\frac{\overline{\omega} + \overline{k}}{\overline{\omega} - \overline{k}}\Big| + 2\Big]\Big\}; \qquad C = 1 + \frac{1}{2\cos^2\theta_w}. \tag{4.31}$$

This function is negative for $\overline{\omega} \sim 0$ but becomes positive for $\overline{\omega} \gg k$ and features only one positive root for any value of k. The gap is given by

$$\omega_g = m_\nu\Big(1 + \frac{1}{2\cos^2\theta_w}\Big)^{1/2}. \tag{4.32}$$

The group velocity for long-wavelength excitations around this gap is obtained from the general expression (4.29) by setting $\Delta = 0$ and the value of the gap (4.32). A straightforward analysis yields $c_+ = 1/3$.

This situation is very different for $\Delta \neq 0$. The discussion on the values of the gaps in the spectrum of collective excitations in the previous subsection as well as the dispersion relation of long-wavelength excitations in the gapless branch indicates that there are three distinct regions of the parameter Δ with qualitatively different behavior.

1. $\Delta < \Delta_c \sim 1.275\cdots$

In this region the quasiparticle spectrum features two gapped branches and no gapless branch. We denote the dispersion relation for the lowest branch by $\omega^+_<(k)$ and that for the higher branch $\omega^+_>(k)$, respectively.

For $\Delta \ll 1$ the gap for the lowest branch is $\omega^+_<(0) \sim \Delta m_\nu$ whereas the gap for the highest branch is $\omega^+_>(0) \sim m_\nu(1 + \frac{1}{2\cos^2\theta_w})^{1/2}$ (see Fig. 2). For increasing values of k the roots corresponding to the largest gap move to larger values of ω, while the roots corresponding to the lowest gap move to smaller values of ω. The spectrum for the lowest branch terminates at an end point k_e which numerically is found to be $k_e \lesssim \Delta/2$. For $k > k_e$ there are no further roots corresponding to the lowest branch and only the highest branch is available. For $k \gg m_\nu$ the dispersion relation along this remaining branch is found to be

$$\omega_+(k) \sim k + \frac{m_\nu^2}{k}\left(1 + \frac{1}{2\cos^2\theta_w}\right) + \cdots. \tag{4.33}$$

The positive energy roots for $\Delta \ll 1$ are displayed in Fig. 3.

For larger values of $\Delta < \Delta_c$ the behavior is qualitatively similar but with some quantitative differences. The positive energy roots of $D_+(\omega, k, \Delta = 1)$ for several values of k are displayed in Fig. 4.

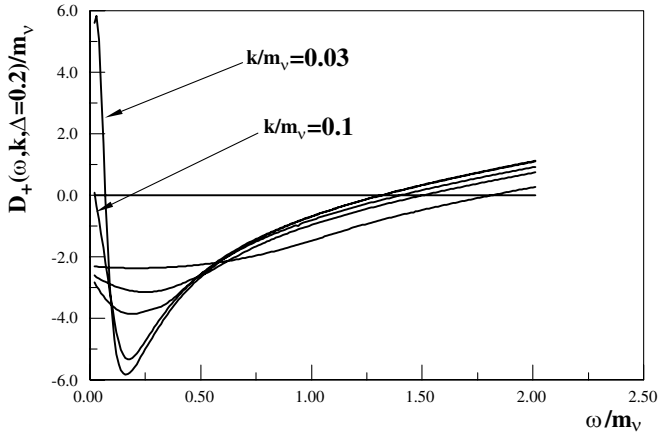

FIG. 3. Roots of $D_+(\omega, k, \Delta = 0.2)/m_\nu$ for $k/m_\nu = 0.03$, 0.1, 0.3, 0.5, 1, respectively.

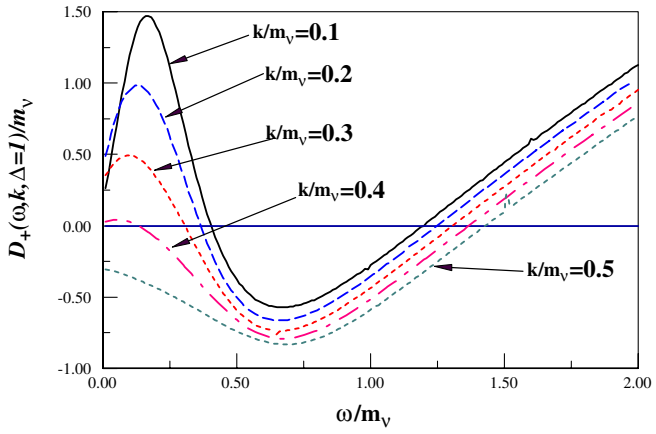

FIG. 4 (color online). Roots of $D_+(\omega, k, \Delta = 1)/m_\nu$ for $k/m_\nu = 0.2$, 0.3, 0.4, 0.5, respectively.

This figure clearly reveals that the branch with the largest gap remains for any value of k, whereas that corresponding to the smallest gap terminates at an end-point value of momentum which numerically is found to be roughly $k_e \lesssim \Delta/2$. For $k > k_e$ there are no *real* roots for the lowest branch.

The weight of the (weakly damped) collective modes to the spectral function is determined by the residue $Z_+(k, \Delta)$ given by Eq. (4.11) evaluated at the position of the root, $\omega_+(k, \Delta)$, which determines the dispersion relation of collective excitations on a particular branch.

The analysis in the previous subsection shows that the function $D_+(\omega, k, \Delta)$ rises sharply for small ω with a slope $\sim 1/\Delta^2$; therefore for $\Delta \ll 1$ the weight of these collective modes with dispersion relation corresponding to the root $\omega^+_<(k, \Delta)$ is

$$Z_+(k, \Delta) \sim \Delta^2 \ll 1. \tag{4.34}$$

Hence for $\Delta \ll 1$ the branch of collective modes with dispersion relation $\omega^+_<(k)$ has *negligible* spectral weight.

We find that for $k \gg m_\nu$, the asymptotic behavior of the collective modes in the upper branch is similar to the HTL limit of unbroken vectorlike theories [17,31,32]. For fast-moving quasiparticles corresponding to the upper branch in the limit $k \gg m_\nu$ the dispersion relation is given by Eq. (4.33) and the spectral weight is found to be

$$Z_+(\omega_+(k), \Delta) \sim 1 - \frac{m_\nu^2}{2k^2}\left(1 + \frac{1}{2\cos^2\theta_w}\right)\ln\left(\frac{2k^2}{m_\nu^2}\right) + \cdots. \tag{4.35}$$

The dispersion relations for both branches together and for the lowest branch separately are displayed in Fig. 5 for $\Delta = 1$.

2. $\Delta_c < \Delta < \pi/2$*: a pitchfork bifurcation of the spectrum*

As discussed above, for $\Delta > \Delta_c = 1.275\cdots$ the only solution of the gap equation is $\omega = 0$; however for

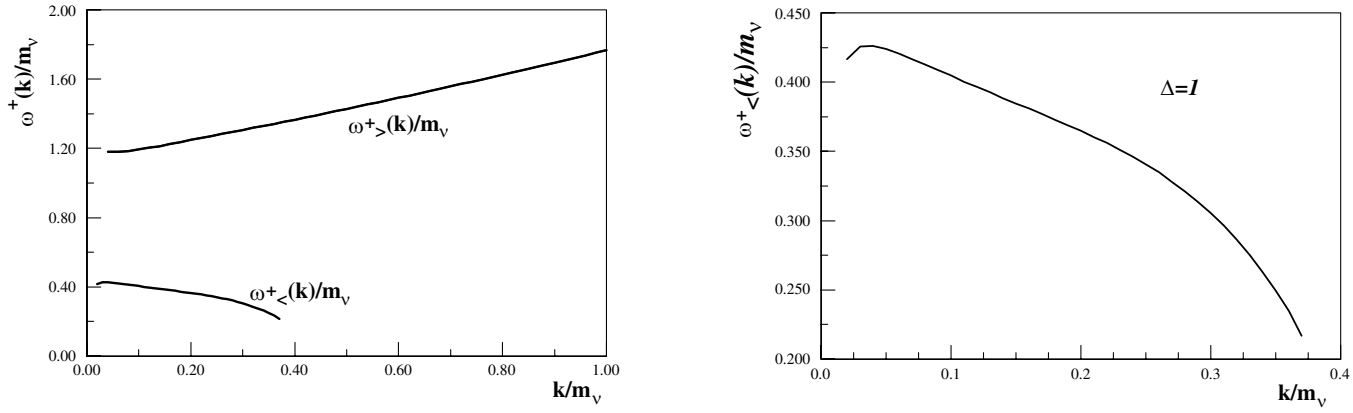

FIG. 5. Left: Dispersion relations for the higher $[\overline{\omega}^{+}_{>}(k)]$ and lower $[\overline{\omega}^{+}_{<}(k)]$ branches of $D_{+}(\omega, k, \Delta = 1)/m_{\nu}$. Right: Lower branch in detail. The lower branch terminates at a value $k_e(\Delta)$; $k_e(1) \sim 0.4$.

$\Delta < \pi/2$ there is no gapless positive energy solution with linear dispersion relation for small k quasiparticles. Therefore the following question arises, what is the nature of the quasiparticle spectrum for $\Delta_c < \Delta < \pi/2$? A numerical study reveals a remarkable answer: for a given value of Δ in this region there is *critical* value of k, denoted by $k_c(\Delta)$ for which *two roots* of the equation $D_{+}(\omega, k, \Delta) = 0$ emerge with a pitchfork bifurcation in the spectrum. This result is depicted in Fig. 6 for $\Delta = 1.4$.

Note in Fig. 6 that there are no roots for $D_{+}(\omega, 0, \Delta = 1.4)$; however two roots emerge continuously for $k > k_c \sim 0.1 m_{\nu}$.

For $\Delta = \Delta_c$ the critical value of the momentum vanishes and becomes nonzero continuously for $\pi/2 > \Delta > \Delta_c$. The critical value $k_c(\Delta)$ determines the origin of the pitchfork bifurcation. One of the branches of the pitchfork bifurcation moves towards larger values of the frequency but the other towards smaller values, eventually terminating at an end point which for the case of Fig. 6 is $k_e \sim 0.5\, m_{\nu}$. For large values of the momenta we find that the roots determine the same dispersion relation as for the previous cases, which is given by Eq. (4.33), and the spectral weight is also given by Eq. (4.35).

While this phenomenon of a pitchfork bifurcation in the spectrum is a noteworthy aspect of neutrino collective excitations in the medium, the narrow window in the parameter Δ within which this phenomenon emerges is rather restricted and without a particular significance within the standard model.

3. $\Delta > \pi/2$

For $\Delta > \pi/2$ only the gapless branch of $D_{+}(\omega, k, \Delta)$ is available and the bifurcated spectrum ends. This is depicted in Fig. 7 which displays the roots near the origin for small values of k/m_{ν}. These roots move continuously towards larger values of the frequency for larger momenta.

The dispersion relation for $\Delta > \Delta_c$ is displayed in Fig. 8 for $\Delta = 3$. For $k \ll m_{\nu}\Delta$ the dispersion relation is linear but *below the light cone* and the group velocity agrees with the result (4.30), whereas for $k \gg m_{\nu}\Delta$ the dispersion

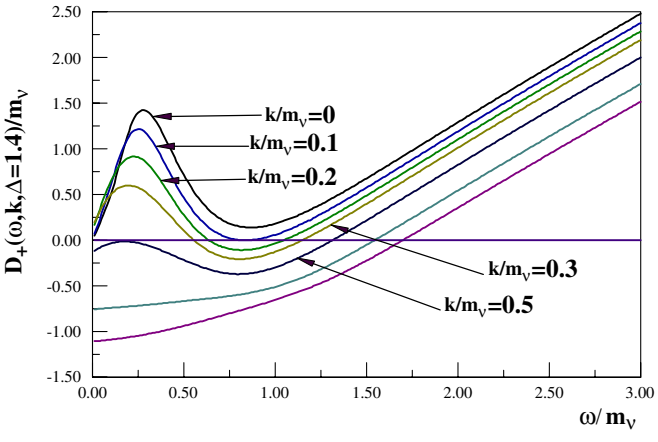

FIG. 6 (color online). Pitchfork bifurcation of the quasiparticle spectrum for $\Delta > \Delta_c$. The function $D_{+}(\omega, k, \Delta = 1.4)/m_{\nu}$ vs ω/m_{ν} for $k/m_{\nu} = 0$, 0.1, 0.2, 0.3, 0.5.

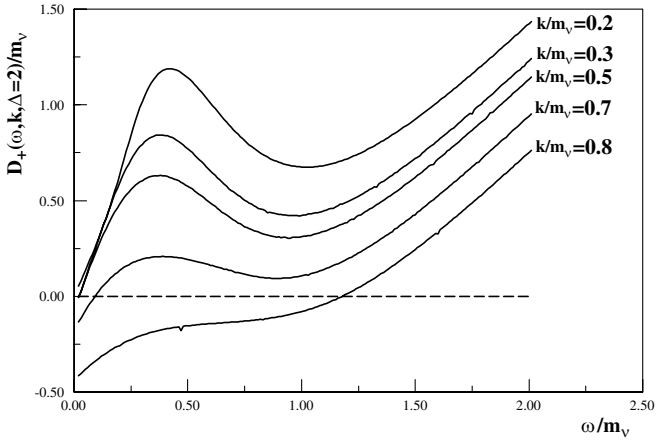

FIG. 7. Emergence of the gapless branch for $D_{+}(\omega, k, \Delta)$ for $\Delta > \pi/2$.

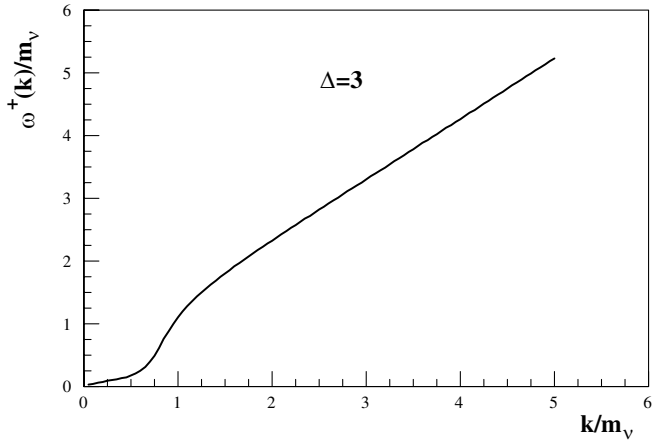

FIG. 8. Quasiparticle dispersion relation for $\Delta = 3$.

relation is found to be

$$\omega^+(k) = k + \frac{m_\nu^2}{k}\left(1 + \frac{1}{2\cos^2\theta_w}\right) + \cdots \qquad (4.36)$$

which is the same as for the large momentum limit of the previous cases. Thus the spectrum interpolates continuously between the soft nonperturbative region $k \ll m_\nu$ and the hard perturbative region $k \gg m_\nu$ with a rapid crossover at $k \approx m_\nu$.

The large momentum limit of the spectral weight in this case is also given by Eq. (4.35).

C. Quasihole spectrum

Just as in the previous section, we begin the analysis by revisiting the case $\Delta = 0$. In this case

$$D_-(\omega, k, 0) = m_\nu\left\{\overline{\omega} + \overline{k} - \frac{C}{2\overline{k}}\left[\left(1 + \frac{\overline{\omega}}{\overline{k}}\right)\ln\left|\frac{\overline{\omega} + \overline{k}}{\overline{\omega} - \overline{k}}\right| - 2\right]\right\};$$
$$C = 1 + \frac{1}{2\cos^2\theta_w}. \qquad (4.37)$$

For $\overline{\omega} = 0$ this function is positive and for $\overline{\omega} \gg \overline{k}$ it has the asymptotic behavior $D_-(\omega, k, 0) \sim \omega$. However for $\omega \sim k$ the logarithm gives rise to a sharp downward spike and the function becomes negative near the light cone for *any* value of k. Therefore the function features *two roots*, one above and one *below* the light cone. The dispersion relation for small k is obtained from Eq. (4.26) for $\Delta = 0$.

As $k \to 0$ the root above the light cone approaches the gap (4.32) from below with group velocity $c_- = -1/3$ and the one below the light cone approaches the origin from above with group velocity $c_- = 1/3$. This is precisely the gapless branch, which is the solution of the gap equation for *any* Δ, including $\Delta = 0$ as mentioned in Sec. IV A. This gapless branch has not been discussed in previous studies of the HTL approximation in unbroken gauge theories [17,31,32] because it is below the light cone and is strongly Landau damped in those cases. We will discuss below the width of collective excitations in this branch (see Sec. IV D).

This simple analysis combined with the linear dispersion relation for long-wavelength collective modes in the gapless branch with *positive energy* roots of $D_-(\omega, k, \Delta)$ indicates that the gapless branch is a solution of $D_-(\omega, k, \Delta) = 0$ for $\Delta < \pi/2$. Positive energy solutions along this branch correspond to gapless quasiholes. For $\Delta \ll 1$ the function $D_-(\omega, k, \Delta)$ has a slope $\propto 1/\Delta^2$ for both the gapless branch and the branch with the smallest gap $\sim\Delta$. Therefore the spectral weight for these branches is of order $\Delta^2 \ll 1$ and therefore negligible with respect to that of the branch with gap $\sim m_\nu(1 + \frac{1}{2\cos^2\theta_w})^{1/2}$.

For $\Delta = 0$ the origin of the two roots, above and below the light cone, is traced to the logarithmic singularity at $\omega = k$ in Eq. (4.37). However inspection of the functions LP and LM given by Eqs. (3.22) and (3.23) reveals that for any $\Delta \neq 0$ this singularity is screened. For small Δ a similar situation featuring two roots is expected for small k. However for larger Δ and k the screening of the light cone singularity will not allow the function to become negative. This feature is clearly displayed in Fig. 9 for $\Delta = 0.2$.

Inspection of this figure reveals the presence of *three* branches as anticipated, two gapped branches and one gapless branch, which is manifest as the root closest to the origin for small values of k in the figure. The gapless branch terminates at an end-point value of the momentum k_e. Figure 9 shows that for larger values of k there are no available roots (see, for example, the curve for $k/m_\nu = 1.5$ in the figure). Therefore for larger values of the momentum all the branches terminate at different end-point values that depend on Δ. It is found numerically that this behavior is

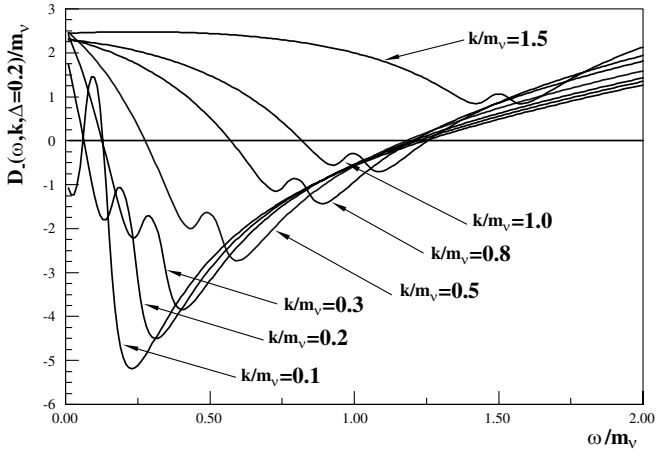

FIG. 9. Roots of $D_-(\omega, k, \Delta = 0.2)/m_\nu$ for $k/m_\nu = 0.1$, 0.2, 0.3, 0.5, 1.0, 1.5, respectively.

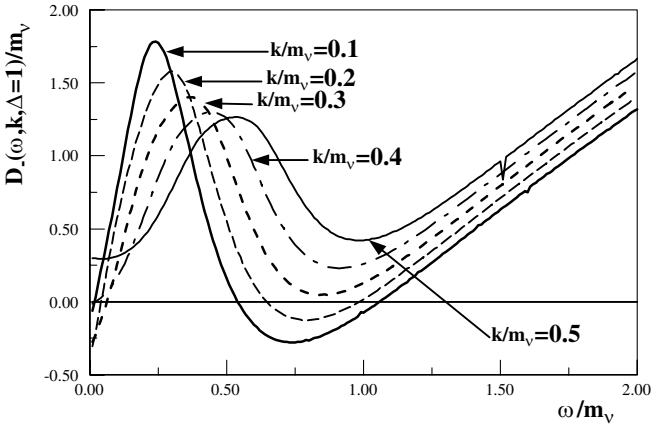

FIG. 10. Roots of $D_-(\omega, k, \Delta = 1)/m_\nu$ for $k/m_\nu = 0.2$, 0.3, 0.4, 0.5, respectively.

consistent for all values of $\Delta < \Delta_c$: one gapless and two gapped branches, each branch terminates at a different end-point value of the momentum which depends on Δ. In particular, the end-point value for the gapless branch diminishes continuously as $\Delta \to \pi/2$. Figure 10 displays the function $D_-(\omega, k, \Delta = 1)$ as a function of ω for several values of k. Three branches are clearly displayed in this figure as well as the termination of these branches at particular values of the momentum k; for example, only the gapless branch remains for $k \gtrsim 0.3 m_\nu$ and finally no roots are available for $k > 0.4 m_\nu$. The quasihole spectrum features end points for all the branches and there are no propagating quasihole states for $k \gg m_\nu$.

Figure 11 display two relevant cases. The left panel shows the function $D_-(\omega, k, \Delta)$ for $\Delta_c < \Delta < \pi/2$. This figure shows that the gapped branches have disappeared and there is a rather small window of (small) momentum within which there are gapless quasihole states. Finally the figure on the right corresponds to $\Delta > \pi/2$, which clearly reveals that there are no available roots and all of the quasihole branches have disappeared, including the gapless branch, consistently with the previous discussion.

In summary, the spectrum of quasihole states features three branches for $\Delta < \Delta_c$, one gapless and two gapped branches; each branch terminates at particular end-point values of the momentum which are functions of Δ. For $\Delta_c < \Delta < \pi/2$ the gapped branches disappear and only the gapless branch remains but terminates at an end-point value of the momentum which is rather small. For $\Delta > \pi/2$ there are no quasihole states. Only for $\Delta \ll 1$ there are quasihole states for $k \gg m_\nu$; this is consistent with the existence of quasihole roots for arbitrarily large k in the $\Delta = 0$ case [17,32].

For generic values of Δ, quasihole states are nonperturbative, soft collective excitations available only for momenta $k \lesssim m_\nu$.

The spectral weight of the quasihole excitations is related to the slope of the function $D_-(\omega, k, \Delta)$ as a function of ω by Eq. (4.11). In the general case the spectral weight must be found numerically; however, inspection of the figures in this section clearly reveals that the spectral weight associated with the gapless excitations is much *smaller* than that of the collective modes on the gapped branches. For $\omega \ll m_\nu$ the slope of the function $D_-(\omega, k, \Delta)$ is $\approx 1/\Delta^2$ for $\Delta \ll 1$. Therefore gapless collective modes yield smaller contributions to the spectral density than the gapped excitations.

D. Damping rates of collective excitations

The damping rates or widths of the quasiparticle and quasihole excitations are given by Eq. (4.12) where $Z_\pm(k)$ are the residues given by Eq. (4.11), and the imaginary parts are given by

$$\mathrm{Im}\, D_\pm(\omega_\pm(k), k) = [\mathrm{Im}\sigma^0_W(k, \omega) \mp \mathrm{Im}\sigma^1_W(k, \omega)] + [\mathrm{Im}\sigma^0_Z(k, \omega) \mp \mathrm{Im}\sigma^1_Z(k, \omega)]. \tag{4.38}$$

The imaginary parts $\mathrm{Im}\sigma^0_{W,Z}(k, \omega); \mathrm{Im}\sigma^1_{W,Z}(k, \omega)$ are given by the expressions (3.9) and (3.10) for the charged

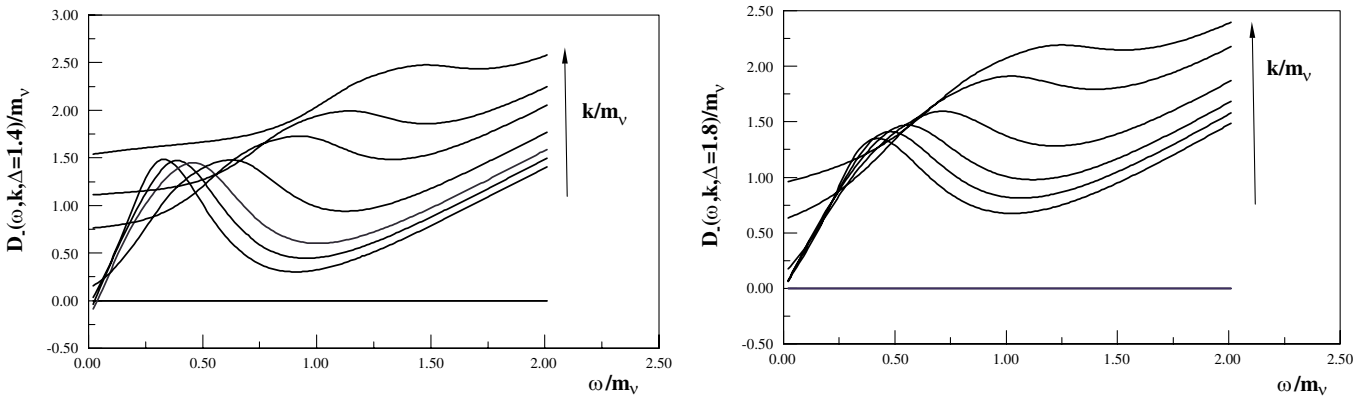

FIG. 11 (color online). Roots of $D_-(\omega, k, \Delta = 1.4)/m_\nu$ and $D_-(\omega, k, \Delta = 1.8)/m_\nu$ for $k/m_\nu = 0.1$, 0.2, 0.3, 0.5, 1, 1.3, respectively. The arrows indicate increasing values of k/m_ν.

current interactions and similar expressions obtained via the replacement (3.7) for the neutral current interactions. An analysis of the delta functions in these expressions determines the region of support of the imaginary parts and thereby establishes whether there is a nontrivial width for the collective excitations with dispersion relations $\omega_{\pm}(k)$.

(i) *Region of support for* $\delta(\omega - p - W_q)$.—This delta function corresponds to the "decay" process $\nu \to W + \bar{l}$ for the charged current and $\nu \to Z + \overline{\nu}$ for the neutral current. Clearly the neutral current contribution cannot be fulfilled. For the charged current contribution, the quasiparticle and quasihole *could* decay provided $m_\nu > M_W(T)$. In principle, the kinematics for this process *could* be satisfied since near the "transition" the mass of the vector boson may be small. However this would entail that

$$gT > M_W(T) \tag{4.39}$$

which, however, contradicts the bounds (5.4) and (5.5) which determine the domain of validity of the perturbative expansion, the latter one being the most conservative. Therefore within the domain of reliability of the perturbative expansion invoked in this study, the kinematics resulting from this delta function cannot be fulfilled on the quasiparticle or quasihole mass shell. The delta function $\delta(\omega + W_q + p)$ has support only for $\omega < 0$ and corresponds to the decay of a negative energy neutrino.

(ii) *Region of support for* $\delta(\omega + p - W_q)$.—This delta function corresponds to the decay process $W \to \nu + \bar{l}$ [the term with $\delta(\omega - p + W_q)$ corresponds to the decay into antineutrino-lepton] and it has support on the neutrino mass shell for $M_W(T) > m_\nu$ for a massless lepton, or $Z \to \nu + \nu$ for $M_Z(T) > 2m_\nu$. Either of the bounds (5.4) and (5.5) which determine the domain of validity of the perturbative expansion guarantees that these processes are kinematically allowed in the region of validity. Therefore this analysis leads to the conclusion that the *decay* of the vector bosons into neutrino-lepton pairs (charged current) or neutrino pairs (neutral current) leads to a *width* for the neutrino collective excitations. These processes are depicted in Fig. 12.

The fact that the decay of vector bosons into neutrinos leads to a width for the neutrino states can be easily understood from a simple kinetic argument. Consider the kinetic equation for the time evolution of the neutrino distribution function. This equation is obtained by a gain minus loss argument as follows. Consider first the charged current interaction: W decay, $W \to \nu\bar{l}$, leads to a gain in the neutrino distribution and the recombination $\nu + \bar{l} \to W$ leads to a loss. The gain and loss terms are obtained from the transition probability per unit time for each process leading to the following kinetic equation:

$$\begin{aligned}\frac{dn_\nu(k)}{dt} = & \int \frac{d^3q}{(2\pi)^3}\frac{|\mathcal{M}_W(q)|^2}{4W_q p} \\ & \times [(1 - n_\nu(k))(1 - n_l(p))N_W(W_q) \\ & - n_\nu(k)n_l(p)(1 + N_W(W_q))] \\ & \times \delta(W_q - p - \omega(k))\end{aligned} \tag{4.40}$$

where $|\mathcal{M}_W(q)|^2$ is the transition probability matrix element, $\vec{p} = \vec{k} - \vec{q}$, and n_l, N_W are the distribution functions for leptons and for vector bosons, respectively. A similar contribution arises for the neutral currents which can be simply obtained from the expression above by the corresponding replacements and $n_l \to n_\nu$. The linearized kinetic equation around the equilibrium distributions is obtained by writing $n_\nu(k) = N_f(k) + \delta n_\nu(k)$ with $N_f(k)$ the Fermi-Dirac distribution function and keeping the lepton and vector boson distribution functions to be those of equilibrium, namely, $n_l(p) = N_f(p); N_W(W_q) = N_b(W_q)$. Keeping only linear terms in $\delta n_\nu(k)$ one obtains the kinetic equation in the relaxation time approximation

$$\begin{aligned}\frac{d\delta n_\nu(k)}{dt} = & -\delta n_\nu(k)\int \frac{d^3q}{(2\pi)^3}\frac{|\mathcal{M}_W(q)|^2}{4W_q p} \\ & \times [N_b(W_q) + N_f(p)]\delta(W_q - p - \omega(k)).\end{aligned} \tag{4.41}$$

Thus we see that the decay rate of the distribution function

$$\begin{aligned}\gamma(k) = & \int \frac{d^3q}{(2\pi)^3}\frac{|\mathcal{M}_W(q)|^2}{4W_q p}[N_b(W_q) + N_f(p)] \\ & \times \delta(W_q - p - \omega(k))\end{aligned} \tag{4.42}$$

is identified with last terms in the imaginary parts (3.9) and (3.10). The damping rate for quasiparticles $\Gamma(k)$ is simply related to the relaxation rate of the distribution function as $\gamma(k) = 2\Gamma(k)$ [17,26,32,36]. The fact that the decay of a *heavier* particle implies a width for the light collective modes in a thermal bath has already been recognized in Refs. [36,40].

A simple analysis of the region of support of $\delta(W_q - p - \omega)$ in (3.9) and (3.10) shows that for ω above the light cone ($\omega > k$) the loop momentum integral is restricted to the range $q^+ \leq q \leq q^-$ where

$$\begin{aligned}q^+ &= \left|\frac{M_W^2(T) - (\omega + k)^2}{2(\omega + k)}\right|; \\ q^- &= \frac{M_W^2(T) - (\omega - k)^2}{2(\omega - k)}.\end{aligned} \tag{4.43}$$

We find that the charged current contributions to the imaginary parts are given by

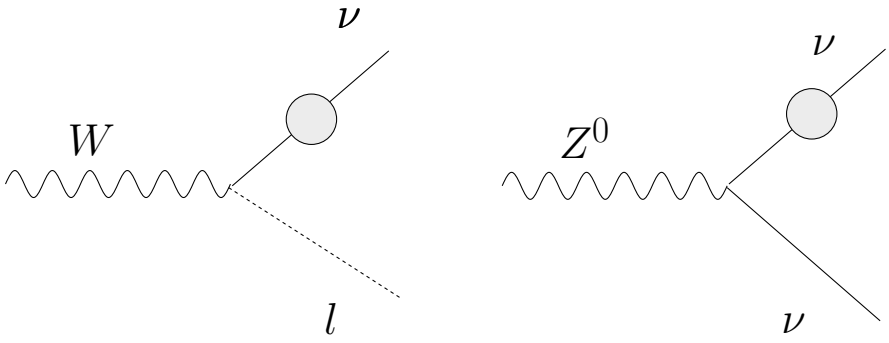

FIG. 12. Decay of vector bosons. $W \to \nu + \bar{l}$ via the charged current or $Z \to \nu\bar{\nu}$ via the neutral currents. The blob in the external neutrino line corresponds to a quasiparticle or quasihole.

$$\mathrm{Im}\, D_{+}^{W}(\omega_{+}(k), k) = \frac{g^2}{32\pi k}\int_{q^-(\omega_{+}(k))}^{q^+(\omega_{+}(k))}\frac{qdq}{W_q}(Q_0(\vec{p}, -\vec{q}) - \hat{\mathbf{k}}\cdot\vec{Q}(\vec{p}, -\vec{q}))[N_f(p) + N_b(W_q)] \tag{4.44}$$

with

$$p = W_q - \omega_{+}(k); \qquad \hat{\mathbf{q}}\cdot\hat{\mathbf{k}} = \frac{q^2 - k^2 - p^2}{2qk} \tag{4.45}$$

and

$$\mathrm{Im}\, D_{-}^{W}(\omega_{-}(k), k) = \frac{g^2}{32\pi k}\int_{q^-(\omega_{-}(k))}^{q^+(\omega_{-}(k))}\frac{qdq}{W_q}(Q_0(\vec{p}, -\vec{q}) + \hat{\mathbf{k}}\cdot\vec{Q}(\vec{p}, -\vec{q}))[N_f(p) + N_b(W_q)] \tag{4.46}$$

with

$$p = W_q - \omega_{-}(k); \qquad \hat{\mathbf{q}}\cdot\hat{\mathbf{k}} = \frac{q^2 - k^2 - p^2}{2qk}. \tag{4.47}$$

The contribution from neutral current interactions is found from the expressions above by the replacement (3.7). The damping rate can be obtained numerically in the general case, but analytic progress can be made in two limits: quasiparticle (quasihole) at rest, namely, $k = 0$, and for fast-moving quasiparticles $T \gg k \gg m_\nu$. As discussed in the previous section, only for $\Delta \ll 1$ are there quasihole states for $k \gg m_\nu$.

Furthermore, within the domain of validity of the perturbative expansion determined by the tighter bound (5.5) it follows that $M_W(T)/m_\nu \gg 1$ which results in several simplifications.

Quasiparticle and quasihole at rest.—For $k = 0$ the damping rates of quasiparticles and quasiholes are the same. It can be obtained directly from the expressions for the imaginary parts (3.9) and (3.10) by recognizing that for $k = 0$ the contribution from (3.10) must vanish by rotational invariance or alternatively by computing the integral in the expressions above in the limit $q^+ \to q^-$. The final result for the damping rate is

$$\Gamma_{\pm}(\omega_g) = \frac{g^2\omega_g}{32\pi}Z[\omega_g]\left[F[M_W(T)] + \frac{F[M_Z(T)]}{2\cos^2\theta_w}\right] \tag{4.48}$$

with

$$F[M] = \left[\frac{M^2 - \omega_g^2}{\omega_g^2}\right]^2\left[1 + \frac{\omega_g^2}{2M^2}\right][N_f(q^*) + N_b(W(q^*))], \tag{4.49}$$

$$q^* = \frac{M^2 - \omega_g^2}{2\omega_g}; \qquad W(q^*) = \frac{M^2 + \omega_g^2}{2\omega_g} \tag{4.50}$$

where ω_g is a nonzero solution of the gap equation (4.20) and $Z[\omega_g]$ is the residue corresponding to zero momentum quasiparticles or quasiholes.

Since $\omega_g \leq m_\nu$ and in the domain of validity of the results $M_{W,Z}(T) \gg m_\nu$, the expression for the function $F[M]$ in Eq. (4.49) simplifies to

$$F[M] \sim \left[\frac{M}{\omega_g}\right]^4\frac{1}{\sinh[M^2/(2\omega_g T)]}. \tag{4.51}$$

Therefore the width for quasiparticles and quasiholes at rest is given by

$$\Gamma_{\pm}(\omega_g) = \frac{2m_\nu}{\pi}Z[\omega_g]\left[\frac{m_\nu}{\omega_g}\right]^3\Delta^2\left\{\frac{1}{\sinh[\Delta(m_\nu/\omega_g)]} + \frac{1}{2\cos^6\theta_w}\frac{1}{\sinh[(\Delta/\cos^2\theta_w)(m_\nu/\omega_g)]}\right\}. \tag{4.52}$$

For $\Delta \ll 1$ the gap for the lowest gapped branch is $\omega_< \sim m_\nu\Delta$ and for the upper branch is $\omega_> \sim m_\nu$ while the residues are $Z[\omega_g] \sim \Delta^2$ for the lower gap and $Z[\omega_g] \sim 1/2$ for the upper branch.

Hence it follows that for $\Delta \ll 1$

$$\Gamma(\omega_<) \approx \omega_<, \tag{4.53}$$

$$\Gamma(\omega_>) \approx \Delta\omega_>. \tag{4.54}$$

Therefore for $\Delta \ll 1$ the lowest branch is strongly damped while the upper branch is weakly damped.

For $\Delta \sim 1; \Delta < \Delta_c$ both the lower and upper branches have gaps of order m_ν (up to factors of order one; see, for example, Fig. 4) and $Z[\omega_g] \sim 1$. Hence for $\Delta < \Delta_c$ but $\Delta \sim 1$,

$$\Gamma(\omega_g) \sim \omega_g \tag{4.55}$$

and collective excitations at rest on either branch are strongly damped.

Fast-moving quasiparticles.—The other limit that is relevant for a comparison with the perturbative results and tractable analytically is that of $\Delta \gtrsim 1$ and fast-moving quasiparticles with $M(T) \gg k \gg m_\nu \Delta$. In this limit only quasiparticles are available since the spectrum of quasiholes terminates at an end point of order $k_e \sim m_\nu \Delta$ for not too small Δ (see Figs. 9–11). For $k \gg m_\nu \Delta$ the quasiparticle dispersion relation is near the light cone and given by Eq. (4.33) and the spectrum of quasiparticles is perturbatively close to the free field spectrum; therefore a comparison to the perturbative results is meaningful.

In this limit $q_+/T \gg 1$ and $q_- \gg M(T)$ the upper limit of the integral can be taken to $q_+ \to \infty$. The remaining integrals are now straightforward and after combining the results from charged and neutral currents we find

$$\Gamma_+(k) \sim \frac{g^2 T}{32\pi} \frac{M_W^2(T)}{k^2} \ln\left[\frac{4k}{m_\nu \Delta}\right]\left(1 + \frac{1}{2\cos^4\theta_w}\right). \tag{4.56}$$

Thus in the limit $k \gg m_\nu \Delta$ quasiparticles are weakly damped since

$$\Gamma_+(k)/k \sim \Delta \frac{m_\nu^3}{k^3} \ln\left[\frac{4k}{m_\nu \Delta}\right] \ll 1. \tag{4.57}$$

V. DOMAIN OF VALIDITY OF THE HTL APPROXIMATION: POSSIBLE CAVEATS

In the HTL approximation we have used the bare propagators for the internal fermion and vector boson lines. Since the HTL approximation relies on loop momentum $q \sim T$ the region of validity of the HTL approximation is determined by the region in which the self-energy corrections to the *internal* lines are perturbative with respect to the loop momentum scale. The study of the previous section indicates that vector boson exchange will lead to a radiative correction to the internal fermionic line yielding a mass scale $m_\nu \sim gT$. Thus the self-energy correction to the lepton or neutrino internal lines is indeed perturbative small in weak coupling.

Furthermore the vector bosons themselves acquire self-energy corrections through fermion loops *and* vector boson loops through the non-Abelian self-interaction. These are displayed in Fig. 13.

The self-energy diagrams with fermion loops [diagrams (c) and (d) as well as similar diagrams with quarks for the neutral vector boson] yield a typical HTL self-energy correction of order g^2T^2 [31,32] and are perturbative for external momentum $q \gg gT$ or for soft external momentum if $M(T) \gg gT$, where $M(T)$ stands generally for the vector boson mass.

These self-energy corrections yield a Debye (electric) mass $m_D \sim gT$ [31–33]. In non-Abelian theories, a magnetic mass $m_m \sim g^2 T$ is also generated at high temperature [31,32].

Since we are considering the high temperature limit with $T \gg M_{W,Z}(T)$ these contributions are perturbative for soft external momentum in the regime

$$T \gg M(T) \gg gT. \tag{5.1}$$

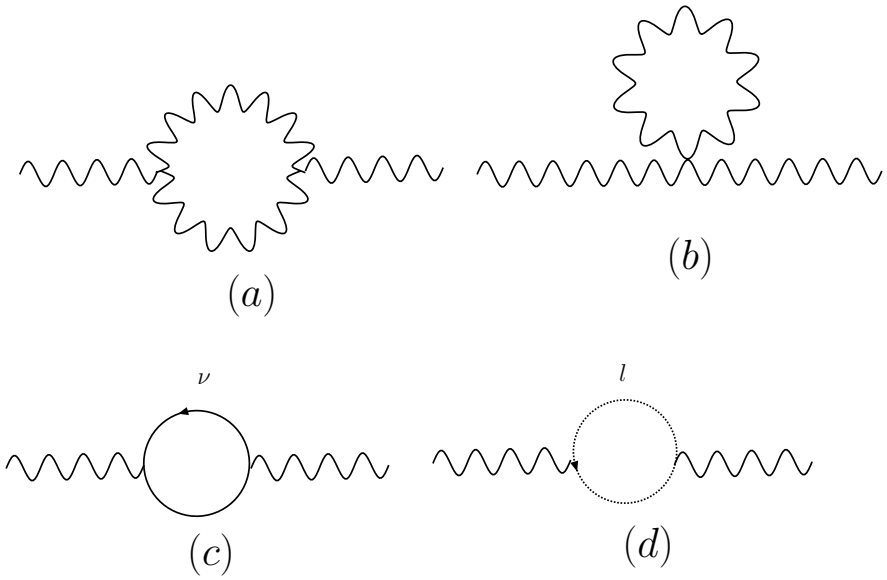

FIG. 13. One-loop diagrams contributing to the self-energy of charged and neutral vector bosons.

A tighter bound emerges from consideration of the self-energy contribution from non-Abelian loops, such as in Fig. 13(a) and 13(b). The HTL power counting [31,32] for these diagrams is modified by the large momentum behavior of the propagators in the (physical) unitary gauge. Since for large momentum the vector boson propagators $G_{\mu\nu}(q) \sim q_\mu q_\nu/q^2M^2(T) \sim 1/M^2(T)$ the *naive* HTL counting assigns a factor of $1/M^2(T)$ for each vector boson line, rather than the usual $1/T^2$ [31,32].

Therefore, according to this modified HTL power counting the vector boson loop with cubic (momentum dependent) vertex in Fig. 13(a) would yield a self-energy contribution

$$\Sigma_a \propto \frac{g^2T^6}{M^4(T)}. \tag{5.2}$$

Four powers of temperature arise from the loop integral with two extra powers from the momentum dependence of each vertex and four powers of M in the denominator because each vector boson line yields a factor $1/M^2(T)$. Similarly the vector boson loop with quartic (momentum independent) vertex in Fig. 13(b), would yield a self-energy contribution

$$\Sigma_b \propto \frac{g^2T^4}{M^2(T)}. \tag{5.3}$$

It is clear that *if* the usual HTL power counting holds for these diagrams as $M(T) \to 0$ the infrared divergences lead to a breakdown of the perturbative expansion, requiring a resummation.

However, for sufficiently high temperatures but *below* the symmetry restoration scale $T_{\rm EW}$, because the standard model features a smooth crossover from the broken to the unbroken "phase," there is a regime for which $T_{\rm EW} > T > M(T)$ within which a perturbative treatment is reliable.

Within this window of validity of perturbation theory, the validity of the HTL approximation will be further bound by the region in which the self-energy contribution to the gauge vector bosons is perturbatively small. The analysis above reveals that for $T \gg M(T)$ Fig. 13(a) gives the largest contribution; since at high temperature the loop momentum is $q \sim T$, the self-energy contribution (5.2) will be perturbative if

$$T > \frac{gT^3}{M^2(T)} \longrightarrow M(T) > g^{1/2}T. \tag{5.4}$$

A tighter and more conservative bound is obtained from the observation that in using the free field theory propagators for the internal lines the dispersion relation of on-shell vector bosons has been used. In particular, the polarization vectors involve the bare mass $\sim M(T)$. Hence a tighter bound is obtained by requiring

$$M(T) > \frac{gT^3}{M^2(T)} \longrightarrow M(T) > g^{1/3}T. \tag{5.5}$$

The bounds above are the result of assuming the validity of the *naive* argument that combines the HTL power counting with the large momentum behavior of the vector boson propagator.

However this simple counting argument ignores the subtleties associated with the underlying gauge invariance as well as potential cancellations. It is *plausible* that the term of $\mathcal{O}(g^2T^6/M^4(T))$ vanishes identically and that there is a cancellation of the terms of $\mathcal{O}(g^2T^4/M^2(T))$ between the diagrams (a) and (b) as a result of Ward identities. *If* such is the case, then only a contribution of $\mathcal{O}(g^2T^2)$ would remain in which case the perturbative expansion is reliable for

$$M(T) \gg gT. \tag{5.6}$$

An indication that these cancellations are *plausible* is found precisely in the neutrino self-energy in the high temperature limit obtained in the appendix and Sec. III. The *naive* HTL power counting combined with the large momentum behavior of the vector boson propagator $\propto 1/M^2(T)$ would lead to the estimate $\sim g^2T^3/M^2(T)$ for the first two terms and g^2T^4/M^2k for the last two terms in the self-energy corrections (3.11) and (3.12). However, remarkable cancellations in both terms lead to $\sim g^2T^2\omega/M^2(T)$ for the first two terms and g^2T^2/k for the last two terms, and perturbation theory is reliable for $M^2(T) \gg gT$. Of course, whether these cancellations also occur in the self-energy of the vector bosons must be studied in detail.

In either of these cases (5.4), (5.5), and (5.6) the vector boson masses from symmetry breaking $M(T)$ are much greater than the Debye or magnetic masses, $m_D \sim gT$, $m_m \sim g^2T$, respectively.

Even if the more conservative bound (5.5) survives deeper scrutiny, within *strict* perturbation theory a regime in which the HTL approximation is reliable within this bound clearly exists, namely, $T > M(T) > g^{1/3}T$. However, this analysis warrants a deeper study of the screening corrections to the vector bosons to provide a reliable bound for the validity of the perturbative expansion at high temperature.

While the HTL approximation is well understood [31,32] in the *absence* of symmetry breaking, the interplay between the generation of Debye and magnetic masses and the mass from symmetry breaking $M(T)$ below the critical temperature is not yet completely understood.

In Ref. [33] the Debye screening correction to the vector boson masses was studied in the temperature regime $M(T) \ll T \ll \sqrt{12}v(0)$, where $v(0)$ is the expectation value of the neutral component of the Higgs doublet *at zero temperature*. At finite temperature it is found in this reference that

$$v(T) = v(0)\left(1 - \frac{T^2}{12v^2(0)}\right). \tag{5.7}$$

Therefore the regime of validity of the HTL approximation as stated in Ref. [33] corresponds to temperatures *much smaller* than the critical temperature.

In this regime of temperature it was found in Ref. [33] that the vector bosons feature a *longitudinal* squared mass of the form

$$M_l^2(T) = M^2(T) + g^2T^2\,\mathcal{A}(\theta_w) \tag{5.8}$$

where $\mathcal{A}(\theta_w)$ is a simple function of the Weinberg angle, and a *transverse* mass squared

$$M_t^2(T) = M^2(T). \tag{5.9}$$

A magnetic mass term is expected at order g^4 [31,32]. These results are valid well below the critical temperature, and to the best of our knowledge there is as yet no clear understanding of the validity of the HTL approximation *near* the critical temperature. Reference [33] concludes by stating that a resummation program must be implemented, a statement that becomes more relevant near the critical temperature. This discussion is meant to bring to the fore the relevant but largely unexplored question of the validity of the HTL near the critical temperature.

Such a study is obviously beyond the realm of this article and is deferred to future investigations.

VI. DISCUSSION OF THE RESULTS

Collective modes.—There are several remarkable differences between the spectrum of collective modes obtained above and those for fermionic collective excitations in QCD or QED [16,17,31,32]. To begin with, in the region in which perturbation theory is reliable, $T \gg M_{W,Z}(T) \gg gT$, the spectrum depends on the mass parameter $m_\nu = gT/4$, which determines the *chirally symmetric gaps* in the spectra, as well as the dimensionless ratio $\Delta = M_W^2(T)/2m_\nu T$ and features, in general, several branches. Gapped branches for quasiparticles and quasiholes are present for $\Delta < \Delta_c \sim 1.275\cdots$; a gapless branch for quasiholes exists for $\Delta < \pi/2$ which becomes a gapless branch of quasiparticles for $\Delta > \pi/2$. The quasihole branches terminate at end points that depend on the value of Δ and for large momentum $k \gg m_\nu\Delta$ there are *no quasihole branches* available. For $\Delta_c < \Delta < \pi/2$ the quasiparticle spectrum features a pitchfork bifurcation with two branches emerging; the one with decreasing frequency terminates at an end point but the other with increasing frequency continues and merges asymptotically with the free field dispersion relation. For $\Delta > \pi/2$ the collective modes are gapless quasiparticles whose dispersion relation lies below the light cone for $k \lesssim m_\nu$ and approaches the free field dispersion relation for $k \gg m_\nu$.

Gauge invariance.—An important aspect that must be discussed is the issue of gauge invariance. We have obtained the neutrino self-energy in the unitary gauge. This is a physical gauge in the sense that it displays only the physical excitations. In any other covariant gauge there are unphysical degrees of freedom, in particular, unphysical Goldstone bosons with a Yukawa coupling to neutrinos. In Ref. [25] the neutrino self-energy (at temperatures much smaller than the mass of the vector boson) was obtained in general covariant gauges and it is shown explicitly that the dispersion relation is independent of the gauge parameter. Furthermore, as discussed explicitly in Refs. [17,31,32] the HTL approximation is gauge invariant. While this body of work clearly points out that the results obtained here are gauge invariant, there is a rather simple argument that makes the gauge invariance manifest up to the one-loop order considered here. In the unitary gauge the only singularities in the Feynman propagators correspond to the on-shell propagation of *physical* degrees of freedom and the unitarity of the S matrix follows directly from the Cutkosky rules [35]. In particular, the imaginary part of the one-loop self-energy can be obtained directly from the Cutkosky rules at tree level, and these only involve the propagation of physical degrees of freedom. Since the full one-loop self-energy is obtained from a dispersion relation, the gauge invariance of the imaginary part guarantees the gauge invariance of the self-energy up to the order considered. For example, the calculation of decay rates in the standard model in the Born approximation in the unitary gauge yields the physical result [35,41], and the imaginary part of one-loop diagrams is obtained from the Born transition elements by the unitarity of the S matrix, which is manifest in the unitary gauge [35] (in fact this *is* the bonus and defining property of the unitary gauge). Therefore we conclude that the results obtained here are manifestly gauge invariant.

Width of collective excitations from vector boson decay.—Another remarkable aspect that must be highlighted is that the width of the neutrino excitations in the medium is a result of the *decay* of the vector bosons into neutrino or neutrino-lepton pairs. This novel mechanism is rather different from the usual collisional relaxation that leads to a width of the quasiparticles. In particular, collisional relaxation results in a width of order G_F^2 since the Born amplitude for such process must necessarily involve the exchange of a vector boson and is therefore of order G_F. In contrast, the width acquired via the decay of a more massive vector boson is of order G_F since the Born amplitude is of order $\sqrt{G_F}$. We emphasize that this mechanism is present even if the vector boson population in the medium is negligible, as can be gleaned from the fact that the term from the imaginary part of the self-energy with support on the mass shell of the neutrino excitation involves $N_f + N_b$. Therefore even if $N_b \sim 0$ there will be a width for the neutrinos if there are fermions (either neutrinos or leptons) in the medium. There is a simple interpretation of this rather striking result, which can be gleaned from the discussion of the width in terms of the kinetic equation (4.40). While the first term in (4.40), which describes the gain in neutrino population from the decay of the vector boson, vanishes

when $N_W \sim 0$, the second term does *not* vanish when $N_W \sim 0$. This second term describes the *recombination* process in which the neutrino in the medium annihilates with either another neutrino (neutral current) or a lepton (charged current) in the medium to produce a vector boson; the *stimulated emission* makes this term nonvanishing even for vanishing population of vector bosons. Therefore this contribution to the width of neutrino excitations will *always* be available in the medium provided the kinematics for energy-momentum conservation is fulfilled. Indeed this is the major restriction for the width that arises from this process; in order for the recombination process to be available, energy-momentum conservation requires that the momentum of the lepton (or neutrino) in the bath must be very large (when the mass of the vector boson is much larger than that of the neutrino quasiparticle or quasihole) and therefore this process will probe the tail of the fermionic distribution function with the ensuing exponential suppression at low temperatures. This novel relaxational mechanism has been previously studied in different contexts in Refs. [36,40].

Comparison with collisional damping—In Refs. [20,26] the *collisional* damping rate of neutrinos was computed up to two-loop order for temperatures much smaller than the vector boson mass. While we cannot directly compare those results to ours for two reasons: (a) our study focuses on temperatures much larger than the (temperature dependent) vector boson mass, (b) we have obtained the damping rate of quasiparticles and quasiholes rather than weakly interacting neutrino states, we can compare the results to obtain at least an estimate of the new effects. The result for the collisional damping rate obtained in Refs. [20,26] is

$$\Gamma_c(\omega) \sim G_F^2 T^4 \omega \tag{6.1}$$

where ω is the energy of the neutrino, and $\omega \sim k$ for a fast-moving neutrino in the medium. In Ref. [27] a similar result for the collisional width was obtained but temperature T replaces the neutrino energy in Eq. (6.1). These results are obtained from a kinetic equation that includes the different scattering contributions, or alternatively as in Ref. [26] from an analysis of the imaginary part of the neutrino self-energy up to two loops. These calculations take the external neutrino to be described by a free field state and are restricted to temperatures below the vector boson mass. Since fast-moving quasiparticles are very similar to the weakly interacting neutrino states, we can proceed to compare the results for the width of the quasiparticle excitations for large momentum $k \gg m_\nu \Delta$ given by Eq. (4.56) with the result of Eq. (6.1) for $\omega \sim k$. The ratio of these results is

$$\frac{\Gamma_+(k)}{\Gamma_c(k)} \sim \frac{1}{4\pi g^2}\left[\frac{m_\nu \Delta}{k}\right]^3 \ln\left[\frac{4k}{m_\nu \Delta}\right]. \tag{6.2}$$

In the expression above we have (unjustifiably) taken the vector boson mass in (6.1) to be equal to $M(T)$ in our calculation, with the purpose of offering a comparison. Granting these caveats, it is clear that under the perturbative assumption $M(T) \gg m_\nu \sim gT$ the ratio $\Gamma_+(k)/\Gamma_c(k) \gtrsim 1$ for $1 \gg (m_\nu \Delta/k) \gtrsim g^{2/3}$. Hence, for a fairly wide range of neutrino energies, the relaxation mechanism via the decay of vector bosons could be comparable to that via collisions. While this comparison must be considered only an estimate (given the caveats mentioned above), it at least *suggests* that the damping mechanism found in this article is competitive with if not larger than the usual collisional relaxation and must be included in treatments of nonequilibrium phenomena of neutrinos in the early Universe.

Regime of validity.—Although the results of Ref. [33] are valid well below the critical temperature, they are encouraging in that the vector bosons acquire a Debye screening mass of order gT which, *if taken at face value near the critical temperature*, would entail that $\Delta \sim g \ll 1$. In this case the dispersion relation of the collective modes will feature the wealth of novel phenomena studied above. *If* further studies confirm that perturbation theory is reliable very near the critical temperature and the vector boson acquires a screening mass of order gT then this would lead to $\Delta \sim g$. Therefore, at least within perturbation theory there is a wide range $1 > \Delta > g$ for which the collective modes feature the most striking and richer aspects of the dispersion relations found above. A similar conclusion is reached if it is required that $M^2(T) > g^4 T^2$ so that the transverse mass is larger than the magnetic mass to avoid the breakdown of perturbation theory at long wavelengths. If, on the other hand, the more stringent constraints (5.4) and (5.5) are shown to be the relevant ones because of infrared phenomena associated with the magnetic mass very near the critical temperature, then $\Delta \gtrsim 1$ and the properties of the collective modes depart perturbatively from those of the vacuum states. It is clear that a further assessment requires a deeper understanding of the validity of the HTL program near the critical temperature.

VII. CONCLUSIONS

Motivated to explore nonequilibrium properties of neutrinos that could impact on thermal leptogenesis, or more generally in neutrino transport in the early Universe, we studied the collective excitations of neutrinos in the standard model at high temperature but below the symmetry breaking scale $T_{\rm EW}$. The main assumption is that the transition from the broken to the unbroken symmetry states in the standard model is either a smooth crossover, as supported by the lattice data with the current bound on the Higgs mass, or of second order. In this scenario the expectation value of the neutral scalar in the standard model vanishes continuously near the transition resulting in that the mass of the vector bosons becomes smaller, which in turn leads to a large population of vector bosons in the thermal bath. We have obtained the spectrum of

collective excitations for standard model neutrinos in the HTL approximation in the regime $T \gg M_{W,Z}(T) \gg gT$ within which perturbation theory is reliable. The excitation spectrum consists of left-handed positive energy negative helicity quasiparticles and left-handed positive energy and positive helicity quasiholes. Antiquasiparticles and antiquasiholes carry negative energy and opposite helicity assignments. The excitation spectrum features a chirally nonbreaking mass scale

$$m_\nu = \frac{gT}{4} \tag{7.1}$$

and depends on the dimensionless ratio $\Delta = M_W^2(T)/2m_\nu T$. For $\Delta < \Delta_c = 1.275\cdots$, the quasiparticle spectrum features two gapped branches and the quasihole spectrum features one gapless and two gapped branches of collective modes.

The lower quasiparticle branch as well as *all* the quasihole branches terminate at particular end-point values of the momentum that depend on Δ. For $\Delta > \pi/2$ only a gapless quasiparticle branch is available, with a dispersion relation that is below the light cone for $k \ll m_\nu$ and asymptotically reaches the free particle dispersion relation for $k \gg m_\nu$.

A novel feature revealed by this study is that the decay of the vector bosons into neutrinos and leptons leads to a damping rate for the neutrino collective modes. A simple kinetic interpretation of this phenomenon was given and analytic expressions for the damping rates were obtained in the limit of small and large momentum of the excitations. These are given by Eqs. (4.48) and (4.56), respectively. For $\Delta \ll 1$ quasiparticles and quasiholes at rest in the lower branch are heavily damped while those in the upper branch are weakly damped, while for $\Delta \gtrsim 1$ all collective modes *at rest* are heavily damped. Fast-moving quasiparticles are weakly damped.

We have compared the damping rate of fast-moving quasiparticles to the results for the collisional damping rate of Refs. [20,26,27] which is a two-loop result $[\mathcal{O}(G_F^2)]$; the ratio is given by Eq. (6.2). The damping rate resulting from vector boson decay at one loop can be *larger* than the collisional relaxation rate in a wide range of neutrino energy.

We have discussed in detail the gauge invariance of the results and assessed the region of validity of the HTL approximation which relies on a strict perturbative expansion.

The novel aspects of the neutrino collective modes near the crossover (or second order) transition to the unbroken phase as well as their nonequilibrium relaxational dynamics studied in this article could be important for a reliable assessment of mechanisms for thermal leptogenesis [12–15].

Further questions.—Clearly an aspect that warrants further study is a more quantitative assessment of the screening corrections to the gauge boson propagators, namely, the diagrams displayed in Fig. 13, in particular, diagrams (a) and (b). A detailed evaluation of these self-energy corrections will yield a better assessment of the domain of validity of the HTL approximation near the critical temperature. At temperatures closer to the transition (or crossover) a resummation of the perturbative series must be invoked in order to correctly treat the infrared divergences in the vector boson propagators [42].

While we have focused on temperatures below the electroweak scale, the study of neutrino collective excitations above this scale is also inherently important for a deeper understanding of early Universe neutrino cosmology. Above this scale, in the phase where the $SU(2) \otimes U(1)$ is restored, new interaction vertices between neutrino, leptons, and the neutral scalar emerge. The contribution from these vertices to the collective excitations and their damping rates is an important future direction of study.

This analysis will require a deeper understanding of the validity of the perturbative expansion as well as the issue of gauge invariance as higher order corrections are contemplated.

Finally, going beyond the standard model, it becomes important to study the effect of these novel phenomena upon neutrino oscillation and, in particular, the possibility of MSW resonances. An intriguing possibility is that of oscillations between different *branches* as well as the competition between the oscillation and relaxation time scales. Furthermore, small neutrino masses will lead to helicity flip transitions which may in turn lead to radiative transitions between the quasiparticle and quasihole branches (or their antiparticles).

These are currently the focus of our current studies on which we expect to report in a forthcoming article [34].

ACKNOWLEDGMENTS

The author thanks the US NSF for support under Grant No. PHY-0242134, and Brad Keister, Adam Leibovich, and Chiu-Man Ho for illuminating conversations and remarks.

APPENDIX: REAL-TIME PROPAGATORS AND SELF-ENERGIES

1. Fermions

For a generic massless fermion field $f(\vec{x}, t)$ the Wightmann and Green's functions at finite temperature are the following:

$$iS^{>}_{\alpha,\beta}(\vec{x} - \vec{x}', t - t') = \langle f_\alpha(\vec{x}, t)\overline{f}_\beta(\vec{x}', t')\rangle = \frac{1}{V}\sum_{\vec{p}} e^{i\vec{p}\cdot(\vec{x}-\vec{x}')} iS^{>}_{\alpha,\beta}(\vec{p}, t - t'), \tag{A1}$$

$$iS^{<}_{\alpha,\beta}(\vec{x}-\vec{x}',t-t') = -\langle \overline{f}_{\beta}(\vec{x}',t') f_{\alpha}(\vec{x},t)\rangle = \frac{1}{V}\sum_{\vec{p}} e^{i\vec{p}\cdot(\vec{x}-\vec{x}')} iS^{<}_{\alpha,\beta}(\vec{p},t-t') \quad \text{(A2)}$$

where α, β are Dirac indices and V is the quantization volume.

The real-time Green's functions along the forward $(+)$ and backward $(-)$ branches are given in terms of these Wightmann functions as follows:

$$\langle f^{(+)}_{\alpha}(\vec{x},t)\overline{f}^{(+)}_{\beta}(\vec{x}',t')\rangle = iS^{++}(\vec{x}-\vec{x}',t-t') = iS^{>}(\vec{x}-\vec{x}',t-t')\Theta(t-t') + iS^{<}(\vec{x}-\vec{x}',t-t')\Theta(t'-t), \quad \text{(A3)}$$

$$\langle f^{(+)}_{\alpha}(\vec{x},t)\overline{f}^{(-)}_{\beta}(\vec{x}',t')\rangle = iS^{+-}(\vec{x}-\vec{x}',t-t') = iS^{<}(\vec{x}-\vec{x}',t-t'). \quad \text{(A4)}$$

At finite temperature T it is straightforward to obtain these correlation functions by expanding the free Fermion fields in terms of Fock creation and annihilation operators and massless spinors. The result is conveniently written in a dispersive form

$$iS^{>}_{\alpha,\beta}(\vec{p},t-t') = \int_{-\infty}^{\infty} dp_0 \rho^{>}_{\alpha,\beta}(\vec{p},p_0) e^{-ip_0(t-t')}, \quad \text{(A5)}$$

$$iS^{<}_{\alpha,\beta}(\vec{p},t-t') = \int_{-\infty}^{\infty} dp_0 \rho^{<}_{\alpha,\beta}(\vec{p},p_0) e^{-ip_0(t-t')} \quad \text{(A6)}$$

where

$$\rho^{>}_{\alpha,\beta}(\vec{p},p_0) = [1-N_f(p_0)]\rho^{f}_{\alpha,\beta}(\vec{p},p_0), \quad \text{(A7)}$$

$$\rho^{<}_{\alpha,\beta}(\vec{p},p_0) = N_f(p_0)\rho^{f}_{\alpha,\beta}(\vec{p},p_0) \quad \text{(A8)}$$

and $N_f(p_0)$ is the Fermi-Dirac distribution function

$$N_f(p_0) = \frac{1}{e^{p_0/T}+1}. \quad \text{(A9)}$$

The free Fermion spectral density is given by

$$\rho^{f}(\vec{p},p_0) = \frac{\not{p}_{+}}{2p}\delta(p_0-p) + \frac{\not{p}_{-}}{2p}\delta(p_0+p), \quad \text{(A10)}$$

$$\not{p}_{\pm} = \gamma^0 p \mp \vec{\gamma}\cdot\vec{p}. \quad \text{(A11)}$$

2. Vector bosons

Consider a generic real vector boson field $A_{\mu}(\vec{x},t)$ of mass M. In unitary gauge it can be expanded in terms of Fock creation and annihilation operators of *physical* states with three polarizations as

$$A^{\mu}(\vec{x},t) = \frac{1}{\sqrt{V}}\sum_{\lambda}\sum_{\vec{k}}\frac{\epsilon^{\mu}_{\lambda}(\vec{k})}{\sqrt{2\omega_k}}[a_{\vec{k},\lambda}e^{-i\omega_k t}e^{i\vec{k}\cdot\vec{x}} + a^{\dagger}_{\vec{k},\lambda}e^{i\omega_k t}e^{-i\vec{k}\cdot\vec{x}}]; \quad \text{(A12)}$$

$$k^{\mu}\epsilon_{\mu,\lambda}(\vec{k}) = 0$$

where $\omega_k = \sqrt{k^2+M^2}$ and k^{μ} is *on-shell* $k^{\mu} = (\omega_k, \vec{k})$. The three polarization vectors are such that

$$\sum_{\lambda=1}^{3}\epsilon^{\mu}_{\lambda}(\vec{k})\epsilon^{\nu}_{\lambda}(\vec{k}) = P^{\mu\nu}(\vec{k}) = -\left(g^{\mu\nu}-\frac{k^{\mu}k^{\nu}}{M^2}\right). \quad \text{(A13)}$$

It is now straightforward to compute the Wightmann functions of the vector bosons in a state in which the physical degrees of freedom are in thermal equilibrium at temperature T. These are given by

$$\langle A_{\mu}(\vec{x},t)A_{\nu}(\vec{x}',t')\rangle = iG^{>}_{\mu,\nu}(\vec{x}-\vec{x}',t-t'), \quad \text{(A14)}$$

$$\langle A_{\nu}(\vec{x}',t')A_{\mu}(\vec{x},t)\rangle = iG^{<}_{\mu,\nu}(\vec{x}-\vec{x}',t-t') \quad \text{(A15)}$$

where $G^{<,>}$ can be conveniently written as spectral integrals in the form

$$iG^{>}_{\mu,\nu}(\vec{x}-\vec{x}',t-t') = \frac{1}{V}\sum_{\vec{k}} e^{i\vec{k}\cdot(\vec{x}-\vec{x}')} \times \int_{-\infty}^{\infty} dk_0 e^{-ik_0(t-t')}[1+N_b(k_0)] \times \rho_{\mu\nu}(k_0,\vec{k}), \quad \text{(A16)}$$

$$iG^{<}_{\mu,\nu}(\vec{x}-\vec{x}',t-t') = \frac{1}{V}\sum_{\vec{k}} e^{i\vec{k}\cdot(\vec{x}-\vec{x}')} \times \int_{-\infty}^{\infty} dk_0 e^{-ik_0(t-t')}N_b(k_0) \times \rho_{\mu\nu}(k_0,\vec{k}) \quad \text{(A17)}$$

where

$$N_b(k_0) = \frac{1}{e^{k_0/T}-1} \quad \text{(A18)}$$

and the spectral density is given by

$$\rho_{\mu\nu}(k_0,\vec{k}) = \frac{1}{2\omega_k}[P_{\mu\nu}(\vec{k})\delta(k_0-\omega_k) - P_{\mu\nu}(-\vec{k}) \times \delta(k_0+\omega_k)]. \quad \text{(A19)}$$

In terms of these Wightmann functions the real-time correlation functions along the forward and backward time branches are given by

$$\langle A^{(+)}_{\mu}(\vec{x},t)A^{(+)}_{\nu}(\vec{x}',t')\rangle = iG^{>}_{\mu,\nu}(\vec{x}-\vec{x}',t-t')\Theta(t-t') + iG^{<}_{\mu,\nu}(\vec{x}-\vec{x}',t-t')\Theta(t'-t), \tag{A20}$$

$$\langle A^{(+)}_{\mu}(\vec{x},t)A^{(-)}_{\nu}(\vec{x}',t')\rangle = iG^{<}_{\mu,\nu}(\vec{x}-\vec{x}',t-t'). \tag{A21}$$

For the charged vector bosons the correlation functions can be found simply from those of the real vector boson fields described above by writing the charged fields as linear combinations of *two* real fields $A^{1,2}$, namely,

$$W^{\pm}_{\mu}(\vec{x},t) = \frac{1}{\sqrt{2}}(A^{1}_{\mu}(\vec{x},t) \pm iA^{2}_{\mu}(\vec{x},t)). \tag{A22}$$

It is straightforward to find the correlation function

$$\langle W^{+}_{\mu}(\vec{x},t)W^{-}_{\mu}(\vec{x}',t')\rangle = G^{>}_{\mu\nu}(\vec{x}-\vec{x}',t-t') \tag{A23}$$

and similarly for the other necessary Wightmann and Green's functions.

3. Retarded self-energies

The diagrams for the one-loop retarded self-energy from charged current interactions are displayed in Fig. 14. A straightforward calculation yields for the charged current contribution the following result:

$$\Sigma^{\rm CC}_{\rm ret}(\vec{x}-\vec{x}',t-t') = \frac{ig^2}{2}R\gamma^{\mu}[iS^{++}(\vec{x}-\vec{x}',t-t') \times iG^{++}_{\mu\nu}(\vec{x}-\vec{x}',t-t') - iS^{<}(\vec{x}-\vec{x}',t-t') \times iG^{<}_{\mu\nu}(\vec{x}-\vec{x}',t-t')]\gamma^{\nu}L \tag{A24}$$

with

$$R = \frac{(1+\gamma^5)}{2}; \qquad L = \frac{(1-\gamma^5)}{2}.$$

A similar result is obtained for the neutral current contribution to the self-energy by simply replacing $g/\sqrt{2} \to g/2\cos\theta_w$ and $M_W \to M_Z = M_W/\cos\theta_w$.

Using the representation of the fermion and vector boson propagators given above the retarded self-energy (A24) can be written as

$$\Sigma_{\rm ret}(\vec{x}-\vec{x}',t-t') = \frac{i}{V}\sum_{\vec{k}}\int_{-\infty}^{\infty}dk_0 R[\tilde{\Sigma}_W(\vec{k},k_0) + \tilde{\Sigma}_Z(\vec{k},k_0)]Le^{i\vec{k}\cdot(\vec{x}-\vec{x}')} \times e^{-ik_0(t-t')}\Theta(t-t'). \tag{A25}$$

The contributions from charged and neutral vector bosons are given by

$$\tilde{\Sigma}_W(\vec{k},k_0) = \frac{g^2}{2}\int\frac{d^3q}{(2\pi)^3}\int dp_0\int dq_0\,\delta(p_0+q_0-k_0) \times \gamma^{\mu}\rho^{f}(\vec{k}-\vec{q},p_0)\rho^{W}_{\mu\nu}(\vec{k})(\vec{q},q_0) \times \gamma^{\nu}(1-N_f(p_0)+N_b(q_0)), \tag{A26}$$

$$\tilde{\Sigma}_Z(\vec{k},k_0) = \frac{g^2}{4\cos^2\theta_w}\int\frac{d^3q}{(2\pi)^3}\int dp_0\int dq_0\,\delta(p_0+q_0-k_0) \times \gamma^{\mu}\rho^{f}(\vec{k}-\vec{q},p_0)\rho^{Z}_{\mu\nu}(\vec{q},q_0) \times \gamma^{\nu}(1-N_f(p_0)+N_b(q_0)) \tag{A27}$$

where $\rho_{W,Z}(\vec{q},q_0)$ are the vector boson spectral densities given by (A19) with $M \equiv M_{W,Z}(T)$, respectively. It is clear that $\tilde{\Sigma}_{W,Z}(\vec{k},k_0)$ correspond to a vectorlike theory.

Using the integral representation of the function $\Theta(t-t')$ the retarded self-energy can be written in the following simple dispersive form:

$$\Sigma_{\rm ret}(\vec{x}-\vec{x}',t-t') = \frac{1}{V}\sum_{\vec{k}}\int_{-\infty}^{\infty}\frac{d\omega}{2\pi}e^{i\vec{k}\cdot(\vec{x}-\vec{x}')}e^{-i\omega(t-t')} \times R[\Sigma_W(\vec{k},\omega)+\Sigma_Z(\vec{k},\omega)]L, \tag{A28}$$

$$\Sigma_{W,Z}(\vec{k},\omega) = \int dk_0\,\frac{\tilde{\Sigma}_{W,Z}(\vec{k},k_0)}{k_0-\omega-i\epsilon} \tag{A29}$$

where $\epsilon \to 0^+$.

Hence from the above expression we identify

$$\tilde{\Sigma}_{W,Z}(\vec{k},\omega) = \frac{1}{\pi}\,{\rm Im}\Sigma_{W,Z}(\vec{k},\omega). \tag{A30}$$

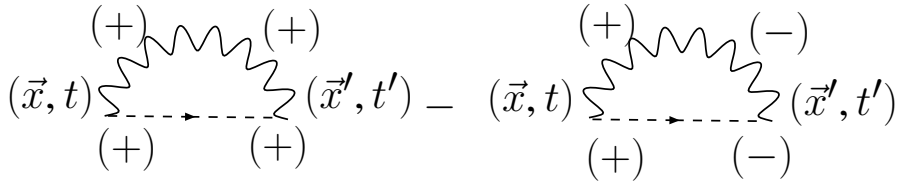

FIG. 14. Retarded self-energy for charged current interactions. The wiggly line is a charged vector boson and the dashed line a lepton. The labels $(\pm)$ correspond to the forward $(+)$ and backward $(-)$ time branches. The corresponding propagators are $iS^{\pm,\pm}(\vec{x}-\vec{x}',t-t')$ and $iG^{\pm\pm}_{\mu\nu}(\vec{x}-\vec{x}',t-t')$ for leptons and charged bosons, respectively.

Furthermore, since we are considering massless neutrinos and leptons in the high temperature approximation, the fermionic spectral density is proportional to γ matrices and does not feature the identity matrix or γ^5 [see Eqs. (A10) and (A11)]; therefore there is the following simplification:

$$R[\tilde{\Sigma}_W(\vec{k},\omega)+\tilde{\Sigma}_Z(\vec{k},\omega)]L=[\Sigma_W(\vec{k},\omega)+\Sigma_Z(\vec{k},\omega)]L. \tag{A31}$$

[1] C. W. Kim and A. Pevsner, *Neutrinos in Physics and Astrophysics* (Harwood Academic Publishers, USA, 1993).

[2] R. N. Mohapatra and P. B. Pal, *Massive Neutrinos in Physics and Astrophysics* (World Scientific, Singapore, 1998).

[3] M. Fukugita and T. Yanagida, *Physics of Neutrinos and Applications to Astrophysics* (Springer-Verlag, Berlin, 2003).

[4] G. G. Raffelt, *Stars as Laboratories for Fundamental Physics* (The University of Chicago Press, Chicago, 1996).

[5] T. K. Kuo and J. Pantaleone, Rev. Mod. Phys. **61**, 937 (1989).

[6] A. D. Dolgov, Surv. High Energy Phys. **17**, 91 (2002); Phys. Rep. **370**, 333 (2002); Nuovo Cimento Soc. Ital. Fis. B **117**, 1081 (2003); hep-ph/0109155.

[7] A. de Gouvea, hep-ph/0411274.

[8] M. Prakash, J. M. Lattimer, R. F. Sawyer, and R. R. Volkas, Annu. Rev. Nucl. Part. Sci. **51**, 295 (2001); S. Reddy, M. Prakash, and J. M. Lattimer, Phys. Rev. D **58**, 013009 (1998); M. Prakash, S. Ratkovic, and S. I. Dutta, astro-ph/0403038.

[9] M. Prakash, J. M. Lattimer, J. A. Pons, A. W. Steiner, and S. Reddy, Lect. Notes Phys. **578**, 364 (2001); S. Reddy and M. Prakash, nucl-th/9508009.

[10] D. G. Yakovlev, A. D. Kaminker, O. Y. Gnedin, and P. Haensel, Phys. Rep. **354**, 1 (2001).

[11] M. Barkovich, J. C. D'Olivo, and R. Montemayor, hep-ph/0503113.

[12] M. Fukugita and T. Yanagida, Phys. Lett. B **174**, 45 (1986).

[13] W. Buchmuller, R. D. Peccei, and T. Yanagida, hep-ph/0502169.

[14] W. Buchmuller, P. Di Bari, and M. Plumacher, New J. Phys. **6**, 105 (2004); Ann. Phys. (N.Y.) **315**, 305 (2005); Nucl. Phys. **B665**, 445 (2003); W. Buchmuller, Acta Phys. Pol. B **32**, 3707 (2001); Lect. Notes Phys. **616**, 39 (2003).

[15] G. F. Giudice, A. Notari, M. Raidal, A. Riotto, and A. Strumia, Nucl. Phys. **B685**, 89 (2004).

[16] V. V. Klimov, Sov. J. Nucl. Phys. **33**, 934 (1981).

[17] H. A. Weldon, Phys. Rev. D **26**, 2789 (1982); Phys. Rev. D **40**, 2410 (1989); Physica A (Amsterdam) **158**, 169 (1989).

[18] L. Wolfenstein, Phys. Rev. D **17**, 2369 (1978).

[19] S. P. Mikheyev and A. Yu. Smirnov, Sov. J. Nucl. Phys. **42**, 913 (1985).

[20] D. Notzold and G. Raffelt, Nucl. Phys. **B307**, 924 (1988).

[21] J. F. Nieves, Phys. Rev. D **40**, 866 (1989).

[22] R. Barbieri and A. Dolgov, Nucl. Phys. **B349**, 743 (1991).

[23] K. Enqvist, K. Kainulainen, and J. Maalampi, Nucl. Phys. **B349**, 754 (1991).

[24] J. C. D'Olivo and J. F. Nieves, Int. J. Mod. Phys. A **11**, 141 (1996).

[25] J. C. D'Olivo, J. F. Nieves, and M. Torres, Phys. Rev. D **46**, 1172 (1992).

[26] E. S. Tututi, M. Torres, and J. C. D'Olivo, Phys. Rev. D **66**, 043001 (2002).

[27] K. Enqvist, K. Kainulainen, and M. Thomson, Nucl. Phys. **B373**, 498 (1992).

[28] T. Holopainen, J. Maalampi, J. Sirkka, and I. Vilja, Nucl. Phys. **B473**, 173 (1996).

[29] A. G. Cohen, D. B. Kaplan, and A. E. Nelson, Nucl. Phys. **B349**, 727 (1991); Annu. Rev. Nucl. Part. Sci. **43**, 27 (1993); G. R. Farrar and M. E. Shaposhnikov, Phys. Rev. D **50**, 774 (1994).

[30] F. Csikor, Z. Fodor, P. Hegedus, A. Jakovac, S. D. Katz, and A. Piroth, Phys. Rev. Lett. **85**, 932 (2000); Y. Aoki, F. Csikor, Z. Fodor, and A. Ukawa, Phys. Rev. D **60**, 013001 (1999); F. Csikor, Z. Fodor, and J. Heitger, Nucl. Phys. B Proc. Suppl. **73**, 659 (1999); Phys. Rev. Lett. **82**, 21 (1999).

[31] R. D. Pisarski, Phys. Rev. Lett. **63**, 1129 (1989); E. Braaten and R. Pisarski, Nucl. Phys. **B337**, 569 (1990); **B339**, 310 (1990); J. Frenkel and J. C. Taylor, Nucl. Phys. **B334**, 199 (1990).

[32] M. Le Bellac, *Thermal Field Theory*, Cambridge Monographs on Mathematical Physics (Cambridge University Press, Cambridge, England, 1966).

[33] C. Manuel, Phys. Rev. D **58**, 016001 (1998); *Strong and Electroweak Matter '98*, edited by Jan Ambjorn, Poul Henrik Damgaard, Kimmo Kainulainen, and Kari Rummukainen (World Scientific, Singapore, 1999).

[34] D. Boyanovsky, C. H. Ho, and H. de Vega (to be published).

[35] M. E. Peskin and D. V. Schroeder, *An Introduction to Quantum Field Theory*, Advanced Book Program (Addison-Wesley Publishing Company, Reading, Massachusetts, 1995).

[36] S. Y.-Wang, D. Boyanovsky, H. J. de Vega, D.-S. Lee, and Y. J. Ng, Phys. Rev. D **61**, 065004 (2000); D. Boyanovsky, H. J. de Vega, D.-S.Lee, Y. J. Ng, and S.-Y. Wang, Phys. Rev. D **59**, 105001 (1999).

[37] J. Schwinger, J. Math. Phys. (N.Y.) **2**, 407 (1961); K. T. Mahanthappa, Phys. Rev. **126**, 329 (1962); P. M. Bakshi and K. T. Mahanthappa, J. Math. Phys. (Cambridge, Mass.) **41**, 12 (1963); L. V. Keldysh, JETP Lett. **20**, 1018 (1965); K. Chou, Z. Su, B. Hao, and L. Yu, Phys. Rep. **118**, 1 (1985); A. Niemi and G. Semenoff, Ann. Phys. (N.Y.) **152**, 105 (1984); N. P. Landsmann and C. G. van Weert, Phys. Rep. **145**, 141 (1987); E. Calzetta and B. L. Hu, Phys. Rev. D **41**, 495 (1990); **37**, 2838 (1990);

J. P. Paz, Phys. Rev. D **41**, 1054 (1990); **42**, 529 (1990).

[38] D. Boyanovsky, H. J. de Vega, and R. Holman, in *Proceedings of the Second Paris Cosmology Colloquium, Observatoire de Paris, 1994*, edited by H. J. de Vega and N. Sanchez (World Scientific, Singapore, 1995), pp. 127–215; *Advances in Astrofundamental Physics*, Erice Chalonge Course, edited by N. Sanchez and A. Zichichi (World Scientific, Singapore, 1995); D. Boyanovsky, H. J. de Vega, R. Holman, D.-S. Lee, and A. Singh, Phys. Rev. D **51**, 4419 (1995); D. Boyanovsky, H. J. de Vega, R. Holman, and J. Salgado, Phys. Rev. D **54**, 7570 (1996); D. Boyanovsky, H. J. de Vega, C. Destri, R. Holman, and J. Salgado, Phys. Rev. D **57**, 7388 (1998).

[39] Proceedings of the Second Paris Cosmology Colloguium, Observatoire de Paris, June 1994 (Ref. [38]); Advances in Astrofundamental Physics (Ref. [38]); D. Boyanovsky, H. J. de Vega, R. Holman, and D.-S. Lee, Phys. Rev. D **52**, 6805 (1995).

[40] D. Boyanovsky, K. Davey, and C. M. Ho, Phys. Rev. D **71**, 023523 (2005).

[41] P. Ramond, *Journeys Beyond the Standard Model*, Frontiers in Physics Series (Perseus Books, Cambridge, Massachusetts, 1999).

[42] A. D. Linde, Phys. Lett. B **96**, 289 (1980); D. Gross, R. Pisarski, and L. Yaffe, Rev. Mod. Phys. **53**, 43 (1981).